Experimental Investigation of Perforated Glazed Transpired Solar Air Heaters

Roozbeh Vaziri

Submitted to the
Institute of Graduate Studies and Research
in partial fulfillment of the requirements for the degree of

Doctor of Philosophy
in
Mechanical Engineering

Eastern Mediterranean University
October 2016
Gazimağusa, North Cyprus

Approval of the Institute of Graduate Studies and Research

Prof. Dr. Mustafa Tümer
Acting Director

I certify that this thesis satisfies the requirements as a thesis for the degree of Doctor of Philosophy in Mechanical Engineering.

Assoc. Prof. Dr. Hasan Hacişevki
Chair, Department of Mechanical Engineering

We certify that we have read this thesis and that in our opinion it is fully adequate in scope and quality as a thesis for the degree of Doctor of Philosophy in Mechanical Engineering.

Assoc. Prof. Dr. Mustafa İlkan
Co-Supervisor

Prof. Dr. Fuat Egelioğlu
Supervisor

Examining Committee

1. Prof. Dr. Senol Baskaya
2. Prof. Dr. Melda Çarpınlıoğlu
3. Prof. Dr. Fuat Egelioğlu
4. Assoc. Prof. Dr. Mustafa İlkan
5. Assist. Prof. Dr. Murat Özdenefe

ABSTRACT

In this experimental study, performances of a novel type solar air heater, perforated glazed solar air heater (PGSAH), and a black coloured unglazed transpired solar air heater (UTSAH) was surveyed. The current study involves two series of experiments. The first series of experiments are accomplished on single pass perforated glazed solar air heaters (SPGSAHs) with different inner colours which have no absorber plates inside the collectors. The second series of experiments have been carried out on double pass perforated glazed solar air heater with packed beds (DPGSAHPB) which are used as absorber plates. The thermal performances of SPGSAH having different inner collector colours, DPGSAH with packed beds and UTSAH were investigated experimentally in this study. Moreover, in order to compare the performances of the PGSAHs and UTSAH, two PGSAHs having perforated plexiglas glazing were constructed and a UTSAH with black coloured perforated sheet metal utilized as an absorber plate was constructed. The diameters of the holes of plexiglas covers and sheet metal cover were 3 mm and the pitch distance was 30 mm. The fans sucked ambient air into the collectors through the perforated plexi glass in the PGSAHs. The thermal efficiency and outlet temperature of collectors were obtained between various mass flow rates of 0.014 and 0.036 kg/s. It was inferred from results that highest value of thermal efficiency and temperature differences were obtained using green and black PGSAHs in first series of experiments and DPGSAH which utilizes iron wools as packing material in second series of experiments. The results indicated that the thermal efficiencies of UTSAHs were lower than the PGSAHs thermal efficiencies. The maximum values of thermal efficiencies for black, green, blue, red,

violet, light yellow and white SPGSAHs are found 85%, 84%, 76%, 65%, 61%, 54% and 55% respectively, at same mass flow rate, the highest thermal efficiency for UTSAH was 50%. Moreover, the average thermal efficiency for DPGSAH with iron wools and DPGSAH with mesh layers are 81.9 %, 75% respectively for air mass flow rate 0.036 kg/s. The highest temperature differences (ΔT) observed were 17.9℃, 17.3℃, 15.4℃ for black, green and blue SPGSAHs respectively for air mass flow rate of 0.024 kg/s. Furthermore, the maximum ΔT for DPGSAH with iron wools is obtained around 29.1℃ at a minimum mass flow rate of 0.014 kg/s. Within specified range of air mass flow rates from 0.014 to 0.036 kg/s, the thermal efficiency of PGSAH enhanced when the air flow rate was increased. As expected, the results demonstrate that thermal efficiencies of PGSAHs were increased if packed bed materials were employed or the collectors were painted by dark colours. The thermal efficiency and outlet air temperature of the DPGSAHPB was greater than the SPGSAH for the same mass flow rates. The DPGSAHPB which utilizes iron wools as packing material had better thermal performance than the DPGSAHPB with mesh layers used as packing material.

Keywords: Renewable energy**,** perforated glazed solar air heater, transpired solar air heater, double pass, thermal efficiency, collector colours

ÖZ

Bu deneysel çalışmada, yeni tip bir güneşli hava ısıtıcısı, delikli geçirgen örtülü güneş hava ısıtıcısı ve siyah renkli delikli yutuculu geçirgen örtüsüz güneş hava ısıtıcısının performansları araştırılmıştır. Bu çalışma iki dizi deney içermektedir. Deneylerin ilk serisi tek geçişli, delikli geçirgen örtülü, farklı kollektör renkleri olan ve yutucu plakası olmayan güneş hava ısıtıcılarında gerçekleştirildi. İkinci deney serisi, çift geçişli delikli geçirgen örtülü, yutucu plaka yerine dolgu malzemesi kullanılan güneş hava ısıtıcıları için gerçekleştirildi. Bu çalışmada tek geçişli delikli geçirgen örtülü, farklı renkli kollektörleri olan hava ısıtıcıları ve çift geçişli delikli geçirgen örtülü, yutucu plaka yerine dolgu malzemesi kullanılan güneş hava ısıtıcılarının ısıl performansları deneysel olarak incelenmiştir. Ayrıca, delikli geçirgen örtülü güneş hava ısıtıcısıları ve siyah renkli delikli yutuculu geçirgen örtüsüz güneş hava ısıtıcısının performanslarını kıyaslamak için, iki adet delikli pleksiglas örtülü güneş hava ısıtıcısı ve yutucusu delikli siyah metal levha örtü olan geçirgen örtüsüz bir adet hava ısıtıcısı üretildi. Plexiglas ve metal levha üzerindeki delik çapları üç mm, delikler arasındaki mesafe 30 mm idi. Dış hava sürekli olarak delikli pleksiglastan kollektör içerisine fan ile emildi. Değişen hava kütle akış hızlarında 0.014 - 0.036 kg/s kollektörlerin ısıl verimlilikleri ve hava çıkış sıcaklıkları elde edildi. Birinci deney serisinde en yüksek ısıl verimlilik ve hava çıkış sıcaklığı kollektörleri siyah ve yeşil olan delikli pleksiglas örtülü güneş hava ısıtıcılarında elde edildi. İkinci deney serisinde en yüksek ısıl verimlilik ve hava çıkış sıcaklığı demir yünü dolgulu çift geçişli delikli pleksiglas örtülü güneş hava ısıtıcısında elde edildi. Sonuçlar siyah renkli delikli yutuculu geçirgen örtüsüz güneş hava ısıtıcılarının ısıl verimliliği, delikli geçirgen örtülü güneş

hava ısıtıcısılarına göre daha az olduğunu göstermektedir. Kollektörleri siyah, yeşil, mavi, kırmızı, mor, açık sarı ve beyaz olan tek geçişli delikli pleksiglas örtülü güneş hava ısıtıcısında elde edilen en yüksek ısıl verimlilik 0.036 kg/s hava akış hızında sırasıyla, %85, %84, %76, %65, %61, %54 ve %55 idi, aynı hava akış hızında siyah renkli delikli yutuculu geçirgen örtüsüz güneş hava ısıtıcılarının ısıl verimliliği %50 idi. Ayrıca, çift geçişli delikli pleksiglas örtülü demir yünü dolgulu ve tel örgü katmanlı güneş hava ısıtıcılarında ortalama verimlilik 0.033 kg/s hava akış hızında sırasıyla %81.9 ve %75 idi. Tek geçişli delikli pleksiglas örtülü siyah, yeşil ve mavi kollektörlü güneş hava ısıtıcılarında elde edilen en yüksek ani sıcaklık değişimi 0.014 kg/s hava akış hızında sırasıyle 17.9 ℃, 17.3 ℃, 15.4 ℃ idi. Ayrıca, demir yünü dolgulu çift geçişli delikli pleksiglas örtülü güneş hava ısıtıcısında elde edilen en yüksek ani sıcaklık değişimi 0.024 kg/s hava akış hızında yaklaşık 29.1℃ idi. Belirtilen 0.014 - 0.036 kg/s hava akış hızı aralığında, delikli geçirgen örtülü güneş hava ısıtıcılarının ısıl verimliliği hava akış hızının artırılması ile artmaktadır. Beklendiği gibi delikli geçirgen örtülü güneş hava ısıtıcılarının kollektörlerinin koyu renkli olması veya kollektörde dolgu malzemesinin kullanılması ısıl verimliliği artırmaktadır. Aynı hava hızlarında çift geçişli delikli pleksiglas örtülü malzeme dolgulu güneş hava ısıtıcısında elde edilen ısıl verimlilik ve ani sıcaklık değişimi tek geçişli delikli pleksiglas örtülü güneş hava ısıtıcısından elde edilenden daha yüksektir. Çift geçişli delikli pleksiglas örtülü demir yünü malzeme dolgulu güneş hava ısıtıcısının ısıl verimliliği tel örgü katmanlı güneş hava ısıtıcısından daha yüksektir.

Anahtar Kelimeler: Yenilenebilir enerji, güneş hava ısıtıcısı, delikli geçirgen örtülü güneş hava ısıtıcısı, ısıl verimlilik, çift geçişli güneş hava ısıtıcısı, kollektör renkleri.

ACKNOWLEDGMENT

I would like to express my sincere gratitude to my supervisor Prof. Dr. Fuat Egelioglu and my co-supervisor Assoc. Prof. Dr. Mustafa İlkan for the continuous support of my PhD study and research. My sincere gratitude also go to the department chair Assoc. Prof. Dr. Hasan Hacişevki for his support, and consideration.

TABLE OF CONTENTS

LIST OF FIGURES

LIST OF SYMBOLS OR LIST OF ABBREVIATIONS

A	Area, (m^2).
A_c	Surface area of collector, (m^2).
C_p	Specific heat of air, (kJ/kg.K).
d	Depth of the collector, (m).
D_h	Hydraulic diameter, (m).
d_w	Wire diameter of screen, (m).
G	Mass velocity, ($kg/s.m^2$).
h	Heat transfer coefficient, $W/(m^2.K)$.
I	Solar radiation, (W/m^2).
k	Thermal conductivity, $W/(m^2.K)$.
L	Length of the collector, (m).
M	Mass, (kg).
$\dot{m}$	Mass flow rate of air, (kg/s).
Nu	Nusselt number.
P_t	Pitch of wire mesh, (m).
P	Prandtl number.
Q	Volumetric flow rate, (m^3/s).
Re	Reynold's number.
r_H	Hydraulic radius.
St	Stanton number.
T	Temperature, (°C).

U_b	Back loss coefficient, W/(m^2. K).
V	Velocity, m/s.
w	Width of the collector, (m).

Greek symbols

α	Absorptivity.
τ	Transmissivity.
φ	Porosity.
η	Thermal efficiency of SAH.
ε	Emissivity.
ρ	Density of air, (kg/m^3).
ΔT	Variation of air temperature (T_{out} - T_{in}), (°C).
ΔT_g	Variation of glass temperature (T_g - T_{in}), (°C).
μ	Dynamic viscosity, (kg/m.s).
ω	Uncertainty.

Subscripts

a	Ambient.
b	Back.
c	Convective.
f	Fluid.
g	Glass.
g1	Interior Glass.
in	Inlet.
m	Mesh layer.
out	Outlet.

r	Radiative
t	Top.
w	Wind.
1	First.
2	Second.

Chapter 1

INTRODUCTION

1.1 Background and Problem Description

Nowadays, energy as a fundamental element of human life is an important global issue for scholars and policymakers. According to the analysis of the US Energy Information Administration (EIA), an institution of the USA federal statistical system, the basic sources of energy were coal 18%, natural gas 27%, petroleum 36%, in 2013.

In 2015, EIA stated that half of USA energy is consumed by space heating in residential and commercial buildings. Based on the official report, the non-fossil sources of energy are divided into renewable 10% and nuclear 8% in 2015 (AEO2015, 2015). In another survey, researchers reported that thermal uses are needed for around 60% of residential sector and about 50% of commercial building energy and almost 33% of whole building energy is allocated to space heating (Ürge-Vorsatz et al., 2015). Admittedly, the main drivers of high energy demand are global population and economic development.

In 2009, Finnish investigators reported that 21% of total energy consumption is dedicated to space heating for public, residential and commercial buildings (Statistics Finland, 2009). Moreover, EU-28 reported that around 40% of total energy is consumed in buildings as the largest sector and also 32%, 26%, 2% of whole energy are utilized for

transportation, industry and agriculture categories respectively in 2012. According to empirical surveys, energy consumption has increased about 1% per year since 1990 for building sector and also 2.4% per year for the sector of electricity at EU level (Odyssee-mure, 2015). In 2013, the investigators illustrated different categories of household energy consumption In USA such as space heating (47%), water heating (26%) and instruments (15%) (economics for energy, 2013). Generally, major sources of energy are none renewable energy because of their availability and cheap procedure of production. Due to several limitations and hazards of fossil fuels consumption for human life and ecosystem, the scholars and policymakers prefer to use the renewable or alternative energy. The huge amount of carbon dioxide (CO_2) that is emitted by burning of fossil as a major greenhouse gas. Nowadays, the greatest challenges of the world are global warming, air pollution, climate change, acid rain and photochemical smog, which are due to fuel combustion (Jesko, 2008). Likewise, a survey conducted on the quantity of the carbon dioxide emissions in building sector in China indicated that amount of carbon dioxide which is emitted by water heating and cooking, and space heating and cooling are around 30% and 40%, respectively (Jing-Li Fan et al., 2015). In the literature, researchers proposed several particular methods to decrease carbon dioxide emissions in space heating. Various international environmental agreements were signed with the aim of protecting the environment and also to reduce CO_2 emission of greenhouse gases and global warming such as the Kyoto Protocol, Vienna convention for the preservation of ozone layer, Montreal protocol on substances that deplete the ozone layer, convention on long-range trans boundary air pollution (CLRTAP) and, United Nations framework convention on climate change (UNFCCC).

Recently, Paris agreement is done within the UNFCCC dealing with greenhouse gases emissions mitigation to stop the increase of global temperature and reduce the harmful effects of climate change (UNFCCC secretariat, 2015). In fact, the policymakers made an agreement on Kyoto Protocol for limiting the greenhouse gases emission. Based on the official report of IEA, heat pumps decreased global CO_2 emissions around 8% (IEA Heat Pump Programme, 2009). However, the goal of the EU is to reduce the emission of greenhouse gases by 20% by 2020 (IEA Heat Pump Centre, 2016). In addition, the amount of renewable energy consumption has increased around 5% since 2000 which is about 14% of total households' consumption in the European countries (Oedysseemure, 2015). In another study, Hanemann et al. (2013) utilized Spanish household detailed data to predict a discrete-continuous model of residential energy demand for heating. EIA predicts that consumption of marketed renewable energy will grow in the sector of electric power and also annual consumption of solar photovoltaic is enhanced by 6.8% per year for next 24 years (AEO2015, 2015). The renewable energy proceeds from natural processes, which are replenished continuously. Basically, solar energy is identified as the basic origin of renewable energy, which harnesses the solar radiation. The sun emits radiant energy, solar radiation, with a wide range of wavelengths from ultraviolet as a short wavelength to infrared as a long wavelength. The amount of incoming solar radiation above the atmosphere that is gained by the earth is 174000 terawatts (TW) as determined by Smil in 1991. Almost thirty percent of this amount of solar radiation reflects back to space and the earth's surface and clouds capture the rest. The technologies of solar collectors are divided into passive and active solar collector; the major distinct between them is the way of harnessing and distributing solar energy.

The distinguished privileges of utilization of solar energy are the rise of sustainability, reduction of pollution and global warming and retention the prices of fossil fuel less than otherwise. Furthermore, solar air heaters (SAHs) are utilized as an impressive and useful method to reduce the CO_2 emissions and captured the solar radiations from the sun to create thermal energy for space heating. In addition, several significant parameters such as the type of collector, solar radiation, absorptivity, orientation and air flow rate have a significant effect on the thermal performances of SAHs. However, the SAHs are cheap with minimum maintenance which having no freezing, corrosion or leakage problems when compared with liquid type collectors. Moreover, SAH is influenced by the disadvantage of minimum thermal efficiency (Singh and Dhiman, 2014).

1.2 Purposes of Thesis

In the literature, there are numerous investigations that consider various types of SAHs aiming to achieve higher thermal efficiencies and higher temperature difference. To the best of our knowledge, there is no empirical research on adoption of the SAHs with facade of building aesthetically but there is a strong trend to achieve higher thermal efficiency by implementing simple modifications on the structure of conventional SAHs. In this experimental study, PGSAHs were constructed where perforated plexi glass was utilized as a top cover of PGSAH. The aim of the first part of the study is to consider aesthetics categories of building facades and roofs with the use of coloured SPGSAHs. The aim of the second section of the experimental study is to obtain maximum thermal performance with the utilization of DPGSAHPB where iron wools or mesh layers were used as packing material. In the current study, thermal performance of UTSAH is compared to different types of PGSAHs simultaneously for various mass flow rates.

In short, the main objectives of this research are as follows:

1. To construct and test coloured SPGSAHs and DPGSAHPBs.

2. To eliminate regular absorber plate from solar heating systems.

3. To investigate the influence of utilizing perforated plexi glass on thermal performance of SAH.

4. To perform experiments under the same conditions, to compare the thermal efficiency and temperature difference for PGSAHs and UTSAH simultaneously and propose the most suitable arrangement to reach the maximum thermal efficiency.

5. To modify the aesthetics categories of building facades and roofs by utilizing coloured SPGSAHs.

1.3 Thesis Motivations and Organisation

Generally, regular type of SAH consists of insulated duct for hot air, air blower and a panel which includes an absorber plate and cover. Because of the low value of convective heat transfer coefficient between the absorber plate and air flow, low amount of thermal efficiency is the main drawback of conventional SAHs. One of the main concern is how to overcome the high amount of heat loss from collectors. The man goal of crent study is to decrease the heat loss from SAH and also to enhance thermal efficiency by increasing of heat transfer area. The organization of the thesis is as follows:

The main objectives of this experimental study are included in Chapter 1. The literature review related to the issue of this investigation has been presented in Chapter 2. The experimental investigations are explained in Chapter 3. Chapter 4 reports the results obtained from the experimental study in detail. The trends of data are shown with diagrams and discussed in depth. Finally, chapter 5 presents the conclusions that have

been derived from this study and also proposes several recommendations for future works. The main goal of current study is to reduce the heat loss through SAH and also to enhance thermal efficiency by increasing of heat transfer area.

Chapter 2

LITERATURE REVIEW

Recently, solar energy has emerged as a leading type of sustainable energy which is utilized to heat the air and water, produce light for buildings and dry agricultural products. As mentioned in the previous chapter, one of the impressive way to decrease greenhouse gases such as CO_2 is solar air heating. In fact, E. Morse proposed and constructed the first type of SAH in 1881 (Kumar and Singh, 2014). The main use of SAH as a solar thermal technology is to convert solar energy to thermal energy. Furthermore, the SAH is utilized in various areas such as commercial, institutional, industrial or residential utilization. SAH are used to create energy between low and moderate temperature.

Among the literature, scholars obtained that the thermal performance of a SAH is affected by various parameters such as orientation, solar radiation, temperature of ambient air, absorption medium, rate of air flow and type of collector (Singh and Dhiman, 2014).

The passive solar systems are utilized to convert solar radiation to useful heat. Unlike passive solar heating, active solar heating utilizes mechanical and electrical device to increase the conversion of solar energy to heat and electric power. Active solar heating is a more involving procedure than passive solar heating which produces higher amount

of heat than a passive system. During the last decade, researchers have accomplished various types of surveys to decrease heat loss while thermal efficiency is increased, which is possible by increase of heat transfer area and turbulence in the flowing channel. In several surveys, scholars reported that collector cover, the pattern of airflow inside the duct, the absorber plate and height of collector are important parameters to impact on thermal performance (Aboul-Enein et al., 2000; Gupta and Kaushi, 2008).

2.1 Different Types of Solar Air Collectors

The SAH, as a heat exchanger, captures solar radiation and converts it to heat for specified area (Bansal et al., 1983). In fact, SAH has some privileges than solar water heater such as less corrosion, no extra fluid loop, no boiling and freezing. On basis of various configurations, the SAHs are categorized to transpired and untranspired solar collectors.

2.1.1 Unglazed Air Collectors or Transpired Solar Collectors

Through the literature review, the most regular type of unglazed solar collector is transpired solar collector (TSC) which includes an absorber without utilization of glass or glazing as a cover of collector. The unglazed transpired solar collector (UTC) were proposed by John Hollick and Rolf Peter; these are utilized to preheat ventilation air for buildings (Hollick, 1994; Kutscher, 1996) (Figure 1).

In another study, Christensen et al., (1990) compared three type of heating systems which included UTC as a novel system. Their results showed that the costs of delivered solar energy are decreased by 70% for the ventilation preheat system in comparison to a conventional solar water heating system. The unglazed air collectors are utilized in agriculture, industrial, commercial and process applications which apply a simple

technology to convert solar radiation to thermal energy by heating air. Furthermore, scholars stated that thermal energy flows are created by natural convection between metal and air flow.

The conventional UTC consists of dark coloured perforated absorber sheets which are installed to a building's south facing the wall to preheat ventilation air. However, air is drawn via the solar heated perforated absorber plate into the building by means of a fan.

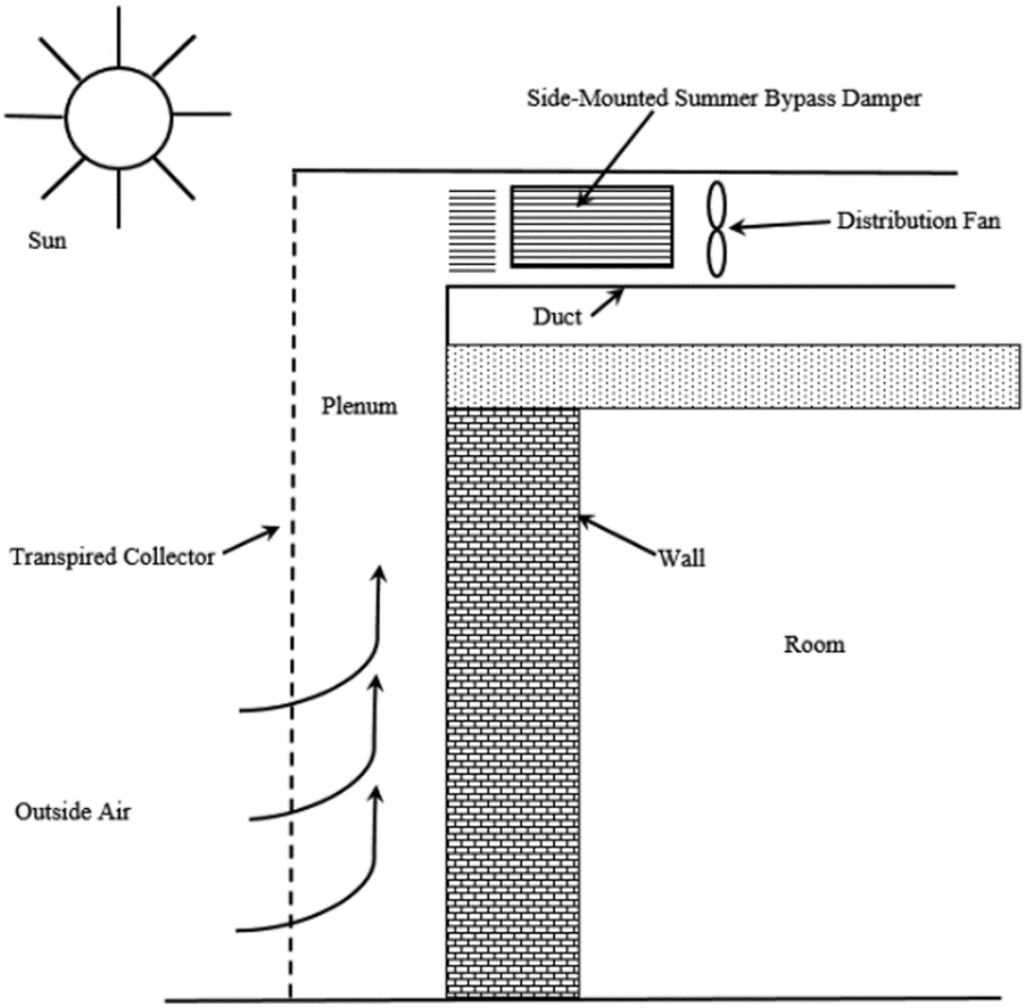

Figure 1: Unglazed Air Collectors or Transpired Solar Collectors (Gholampour.M and Ameri.M, 2014).

The structure of UTCs is more simple and cheaper than glazed collectors. In the literature it was mentioned that UTCs have about 70% efficiency (Cali et al., 1999; Wang et al., 2006). In fact, UTC is the product of a private solar heating and energy conservation company and also National Renewable Energy Laboratory (NREL) as a governmental institution in the USA. NREL (2006) indicated that the ambient air can be preheated by UTC around 22 ℃.

The similar detailed descriptions and assembling of the UTCs can be found in another survey (NREL, 1998; Solar Wall, 2008). In another study, Dymond and Kutscher (1997) proposed a specific model for analysis of TSC. However, Hollick (1998) analyzed the thermal performance of UTC and also illustrated capability of UTCs to preserve the house energy consumption up to $1\frac{\mathrm{MWh}}{\mathrm{m^2.year}}$. In addition, Van Decker et al. (2001) accomplished an investigation on heat exchange effectiveness for UTCs. In fact, the UTCs are appropriate to preheat ventilation air in commercial and industrial buildings that have huge ventilation requirements. In another investigation, Motahar and Alemrajabi (2010) surveyed an exergy analysis of UTC by use of a steady state model. Their study illustrated that radiation and perforation are significant factors that have influenced the thermal performance of heating systems. The UTCs installed perforated metallic absorber plate to the building which creates plenum as an air space between the perforated absorber plate and building. Ambient air is sucked into the plenum through perforated absorber by the use of fan (Kutscher et al., 1993). Sebastien and Suzelle (2011) stated that the perforations of absorber plate permit the ventilation air to remove heat loss with convection from the exterior surface of UTC.

On the basis of a heat balance, a mathematical model is conducted by Gao and Fang (2011). Their results demonstrated that efficiency of collector is influenced by radiation and airflow strongly. In another study, scholars stated that efficiency of UTC could be achieved 80% by air flow of 0.05 m/s (Kutscher CF et al., 1991). Moreover, the collector performance does not affect by wind at this specific speed of air. In winter time, optimum thermal performance is achieved by TSCs which are located on the wall to receiving more solar radiation.

2.1.2 Glazed Solar Collectors

Recently, the glazed solar collectors (GSCs) become more popular among customers for space heating. As shown in Figure 2, the structure of GSC includes transparent material such as plastic or glass to transmit the solar radiation for heat production inside the collector while minimizes convective heat losses to the environment.

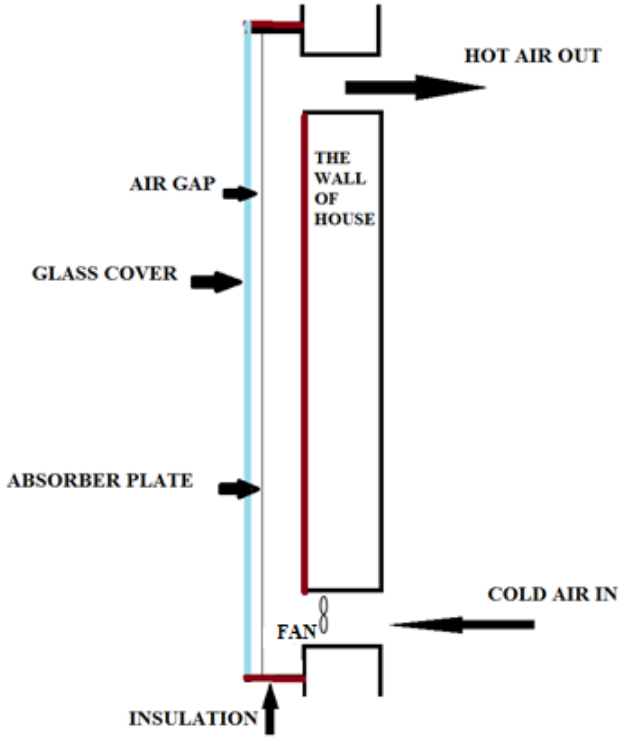

Figure 2: Glazed Air Collectors.

Arulanandam et al. (1997) obtained that proper efficiencies could be gained by utilization of transpired plate absorbers which is made of lower conductivity materials. In addition, SAHs were categorized based on different paths of air flow on an absorber such as through pass, back pass, front pass and integration of front and back pass collectors.

2.1.3 Single- Pass Solar Collectors

The regular structure of a single pass SAH includes a collector with one or double glass utilized on top of the collector (Figure 3). Moreover, the absorber plate is installed inside the collector which is parallel to the transparent cover where air flows between absorber and glazing. Additionally, single pass SAHs are divided into front and back pass SAHs.

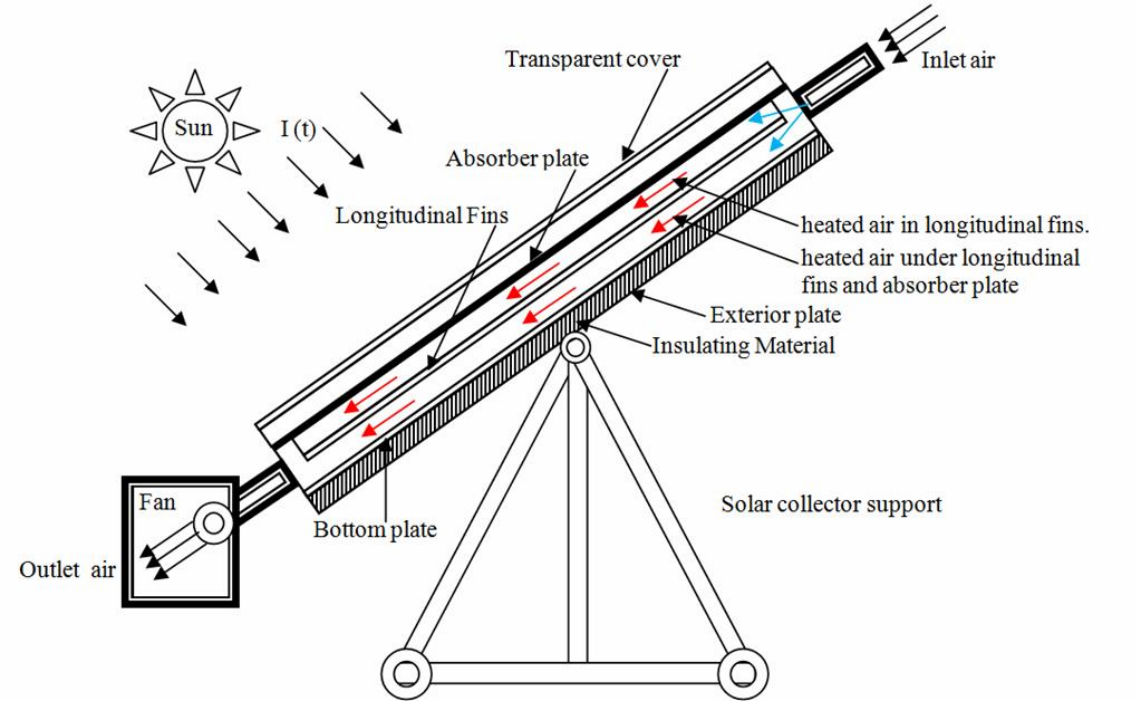

Figure 3: Single Pass SAH (Chabane F. et al., 2013).

Three different types of single pass SAHs are surveyed by Gill et al. (2012) and their results demonstrated that thermal efficiency of single pass SAH by using iron chips as a

packed bed is higher than the other two SAHs. In another experimental study, the thermal performances of three different types of single pass SAHs were investigated where the single pass SAH with trapezoidal obstacles achieved the maximum thermal efficiency in comparison with the other two SAHs (Labed A et al., 2012).

2.1.4 Through-pass Air Collector

The highest thermal efficiency is obtained by through pass air collector which air flows via duct and moves through a sheet (Fig. 4). In addition, air temperature enhances due to the conductive properties of sheet and air convective characteristics.

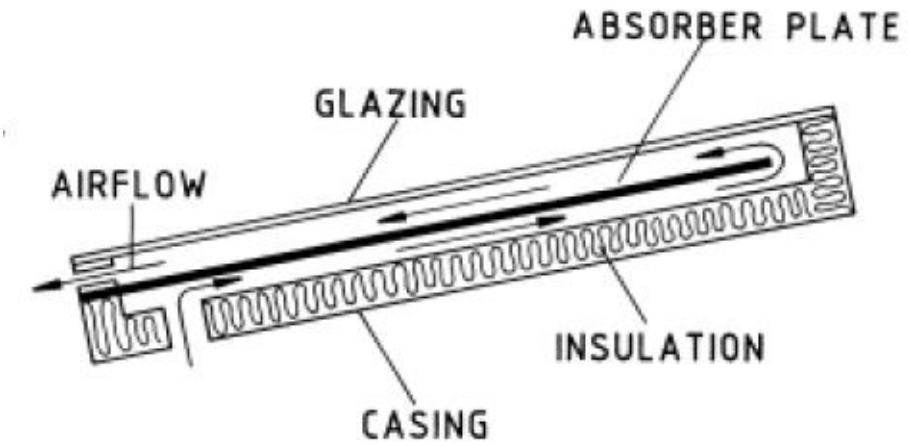

Figure 4: Through Pass Air Collector (Ekenchukwu and Norton, 1999).

2.1.5 Front, Back and Combination Pass Air Heater

The back pass SAH is utilized to enhance air temperature by moving along back of heated solar absorber and they are unglazed and mounted as a part of building facade. However, air is heated by passing over front side of the absorber, between glazing and absorber, in front pass SAH such as glazed double facade. Moreover, the surface area of heat transfer is greater for front and back pass SAH due to moving air on both sides of

heated absorber. In addition, thermal performance of front pass, back pass and combination pass collectors are inappropriate for cold climates due to high amount of heat loss (Figure 5).

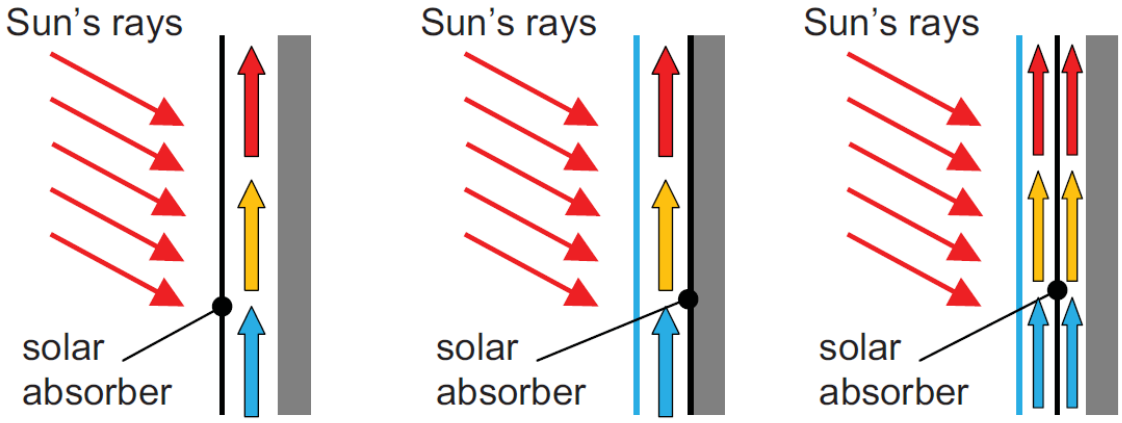

(a) (b) (c)

Figure 5: (a) Back pass (b) Front pass (c) Front and Back Pass Collector (Pavel et al., 2012).

Generally, SAH includes a collector which is constructed of wood or metal, an air blower and an absorber plate, which takes the solar radiation. There are various types of absorber plates such as fins, corrugated, flat and grooved plates. Also, absorber plate could be integrated with the obstacles. Due to reduced convection and radiation heat losses to surrounding, solar air collector should be insulated properly.

2.1.6 Double Glazing Solar Collector

To increase the thermal efficiency of regular SAHs, several modifications were suggested in order to reduce heat losses and also enhances the convection coefficient between air and the absorber plate. Martin and Fjeld (1975) stated that double glazing is used to reduce the convection heat loses from the cover of collector.

Additionally, Aboul-Enein et al. (2000) demonstrated that thermal performance is improved by utilization of double-glass covers which reduces heat loss from the top side of collector to the environment. In another study, Deniz et al. (2012) surveyed three configurations of single pass collectors; a SAH with double glass covers having fins, a SAH without fins and a SAH having fins and single cover. Bahrehmand et. al. (2015) accomplished a mathematical survey on single and double glazing SAHs. Moreover, the results showed that thermal performance of double glazing SAH is higher than single glazed SAH.

2.1.7 Double-Pass Solar Collectors

The absorber plate is located between the cover plate and a layer of insulation for double-pass solar collector and air moves on both sides of absorber plate. Moreover, double pass solar collectors are classified into different types such as parallel pass cover plate solar collector and double pass counter flow solar collector. In another survey, Chamolia et al., (2012) showed that a double-pass SAH has higher thermal efficiency than a single-pass SAH (Chamolia et al., 2012).

In order to increase the thermal efficiency and decrease heat losses, extensive research has been conducted on double pass SAHs having packed bed, extensive surfaces or corrugated absorbers. Furthermore, airflow moves via the upper channel (through the both glass covers) for double pass SAH and the direction of air changes to pass through bottom bed and second glass. Double pass channel was investigated by several researchers, in which the air moves on top and bottom of the absorber plate (Sopian et al., 1999; Yeh et al., 2002; Paisarn, 2005; Ho et al., 2005; Lertsatitthanakorn et al., 2008; Esen, 2008; Ozgen et al., 2009). Alejandro and Jose (2013) proposed two types of

analytical model for thermal performance of double parallel flow SAH and also double pass counter flow SAH. Yeh et al. (2002) suggested double flow SAHs having fins attached to improve thermal efficiency. Moreover, Ho et al. (2005) conducted experiments on a SAH where the absorber plate is situated inside the double pass channel for a flat plate SAH with recycle. Their results indicated that efficiency of collector has remarkable enhancement with utilization of recycle type double pass devices.

Omojaro et al., (2010) investigated experimentally double pass SAHs and they utilized several steel wire mesh layers instead of absorber plate and then longitudinal fins have installed inside SAH. The maximum amount of thermal efficiency of double pass SAH was reported as 63.74% for the mass flow rate of 0.038 kg/s. Deniz et al. (2010) conducted a comparative survey on different types of flat plate SAHs for various mass flow rates, and tilt angles. The results indicated that highest thermal efficiency is obtained by using finned double glass collector.

2.1.8 Solar Collectors with Obstacles

In order to increase heat transfer coefficient inside the collector, various improvements have been proposed such as utilization of finned absorber plates (Yeh et al., 2002; Paisarn, 2005a, b; Lertsatitthanakorn et al., 2008; Esen, 2008; Ozgen et al., 2009; Yeh &Ho, 2009) or situating porous material such as wire mesh screen inside the collector (Mohamad, 1977, Thakur et al., 2003, Qenawy and Mohamad, 2007) limestone and gravels (Ramadan et al., 2007, El-Sebaii et al., 2007). The main aim of using porous media is to enhance the ratio of surface area to unit volume; thus achieving considerable improvement in thermal efficiency. The impact of various configurations, orientation,

roughness inside the collectors on the thermal performance of SAHs have been investigated during decades.

The thermal performance of SAH is enhanced by creating turbulent flow inside the collector which could be conceivable by installing obstacles, ribs, rings, baffles, fins and vortex generator. Moreover, it was shown that ribs, fins, baffles and various combinations of roughness elements are utilized to increase heat transfer coefficient and thermal efficiency of SAHs (Yongsirie et al., 2014; Alam et al., 2014).

The thermal efficiency and effective efficiency are increased for roughened absorber plates SAHs compared with SAHs having smooth absorber plates (Brij&Ranjit, 2012). There was an experimental study on friction properties and heat transfer of a rectangular channel with multiple arc shaped roughness parts on the absorber plate of the SAH (Singh et al., 2014). Their results showed that the highest heat transfer and maximum friction factor were achieved with an attack angle of 60°. In a recent study, researchers surveyed on exergetic performance of a SAH with arc shape oriented as roughness part. It was found that arc shaped protruded SAH is more efficient than smooth regular flat plate SAH for Reynolds number less than 20,000 (Sanjay et al., 2014).

Pottler et al. (1999) suggested an optimization method for SAHs with the flow behind the absorber plate. However, their results showed that SAH having fins with optimal distance between them has highest thermal performance. Mittal and Varshney (2006) conducted thermo hydraulic investigations on black wire mesh SAH and illustrated that thermal efficiency and effective efficiency of these novel collectors are much higher than conventional flat plate collectors. In another investigation, El-khawajah et al. (2011)

conducted experiments on double pass SAHs with various numbers of fins attached and wire mesh layers. Furthermore, they obtained that higher thermal efficiency is achieved as air mass flow rate and number of fins were increased.

The thermal performance of a single pass SAH having five longitudinal fins attached is investigated by Chabane et al. (2014). Their results demonstrated that the maximum values of exit air temperature and collector efficiency are achieved by finned collector. Kumar et al. (2014) investigated the thermal performance of artificial roughed SAH ducts. The single pass and double pass SAHs having four painted dark black transverse fins were presented by Mahmood et al. (2015) and their results showed that higher thermal efficiency is obtained in the double pass SAH. Fudholi et al. (2011) carried out a theoretical study on three types of counter flow SAHs with longitudinal fins attached on top, bottom or on the top and bottom of flat plate absorber. Their survey showed that the number and height of the fins are significant parameters to increase thermal efficiencies of SAHs.

Yeh et al. (2002) investigated specific type of solar collector where an absorbing plate with fins was inserted inside the channel to divide the air passing through the collector into two equal parts. The maximum experimental efficiency was about 70.8% at air flow rate of 77.04 kg/h and good agreement was achieved between experimental data and theoretical solutions.

In another experimental study, the comparison between three different types of single pass SAHs (two of them used different obstacles and one of them utilized no obstacle) was done and then proper comparison was compared with double pass solar bed having

the same type of obstacles. Their results demonstrated that double pass SAH having trapezoidal obstacles improves thermal performance (Adnane et al., 2012).

Additionally, scholars found that the turbulence of airflow via a duct will be enhanced by the use of baffles and obstacles. Their results determined that there is a positive influence on heat transfer by utilization of artificial obstacle surface (Saxena et al., 2015). Pottler et al. (1999) proposed an optimization method for SAHs with fins and found that absorber plate with continuous fins have maximum energy gain if the optimal space between the fins is about 5 to 10 mm and the optimum flow regime is laminar.

In order to achieve better thermal efficiency, Yeh et al. (2002) constructed new SAH for double flow operation in SAHs having fins installed on both sides of the absorber plate. Kurtbas and Turgut (2006) stated that free or attached fins which are installed on absorber plates, have remarkable effect on thermal efficiency and exergy loss of SAH. El-Sebaii et al. (2007) investigated the thermal performance of double pass finned plate SAH. Their study showed that the thermal efficiency and exit temperature of double pass v-corrugated plate SAH is higher than the double pass-finned plate SAH.

Hikmet (2008) indicated that flat plate SAH having some obstacles has higher efficiency than SAH without obstacles. In another study, SAHs with metal rib grits roughness are proposed by Karmare and Tikekar (2009) in order to reach the optimum thermohydraulic performance. They stated that thermal efficiency of SAH which utilizes metal rib grits roughness increases significantly. Hans et al. (2010) proposed use of a rectangular duct roughened having multiple v-ribs in SAHs to enhance the heat transfer and friction factor. Akpinar and Koçyiğit (2010) tested four SAHs and analyzed thermal performance of

novel type of flat plate SAH which different obstacles attached on absorber plate and then compared with SAH without obstacles. Their study concluded that maximum thermal efficiency and temperature difference are obtained by SAHs with leaf obstacles and also minimum value of thermal efficiency was achieved by SAH without obstacles. Moreover, three various types of SAHs, two SAHs with fins and SAH without fins, are investigated by Alta et al. (2010). On the basis of their results, thermal efficiency and temperature differences are enhanced by use of more transparent covers and fins. In addition, Giovanni Tanda (2011) reveals that performance of SAH having ribs on absorber plate is more preferable than smooth channel. In another research, investigators surveyed on thermal performance of double pass v-corrugated plate SAH and double pass finned plate SAH (El- Sebaii et al., 2011). They reported that double pass v-corrugated plate SAH has highest efficiency among the other SAHs. Yang et al. (2012) analyzed thermal performance of six types of collectors which were tested simultaneously. Their study illustrated that thermal efficiency is affected by heat transfer resistance of air flow and also transmittance of transparent cover. Bayraka et al. (2013) presented an experimental investigation on SAHs equipped with porous baffles. Their study demonstrated that thermal efficiency of the SAH with obstacles is higher than SAH without obstacle. In another survey, Krishnananth and Murugavel (2013) integrated thermal energy storage with double pass SAH.

2.1.9 Coloured Solar Collectors

Generally, solar collectors with black coloured absorber plates are not deemed compatible aesthetically with the colour of building facades and roofs. Cyprus has become one of the leading countries to utilize solar water heating (Kalogirou S., 1997). However, solar air heating is being ignored due to the architectural unattractiveness of

SAHs to dwellings. Several researchers studied the use of different coloured absorber plates which are adopted to the building's colour. In an experimental investigation, Tripanagnostopoulos et al. (2000) investigated performance of three flat plate solar water collectors having black, blue, red and brown absorbers with and without glazing.

Their results indicated that efficiencies of collectors having blue, red and brown absorber plates are close to flat plate solar water collector with black coloured absorber plate. Moreover, Anderson et al. (2010) conducted an experimental survey on impacts of the colour of absorber plate on thermal performance of building integrated SAH. In fact, the aim of the current study is to construct glazed transpired SAH with different colours of inner collector. Additionally, this investigation compares thermal performance of coloured PGSAHs with UTSAH. Using different coloured panels are more applicable to adjust with the appearance and integration into the buildings which provides a substantial fraction of heating load.

2.1.10 Double pass Solar Collectors with Packed Bed

A comprehensive survey on double pass SAH is conducted by Chamoli et al. (2012). Based on their results, they examined the majority of experimental researches related to double pass SAH having porous media and extended surfaces. The air mass flow rate and packing porosity are significant factors that influence the performance of SAHs. In another study, the packed bed SAH with iron screen matrices was surveyed by Ahmad et al. (1996). Their study showed that efficiency of SAH has increased with enhancement of air mass flow rate and decrease of bed depth to element size ratio and also with reduction of porosity. Varshney and Saini (1998) accomplished several experiments on SAHs having wire mesh screen matrices. Thakur et al. (2003) surveyed on a low porosity

packed bed SAH which included various types of wire screen matrix. Their findings illustrated that volumetric heat transfer coefficient increases by reducing porosity. Mittal and Varshney (2006) presented packed bed SAH having wire screen matrices with various geometrical factors. Their results showed that the thermal performance of packed bed SAH is higher than regular collectors.

El-Sebaii et al. (2007) compared thermal performance of double pass packed bed SAH with regular double pass SAH theoretically and experimentally, the double pass packed bed SAH utilized gravel and limestone as packed bed materials. Their findings showed that there is a substantial improvement in thermal performance when utilizing packed bed in double pass SAH. Furthermore, scholars determined that annual averages of thermal efficiency and exit temperature of air of double pass SAH with gravel were higher than that of regular SAHs. The thermal performance of a double glass and double pass with a packed bed (DPSAHPB) which utilized limestone and gravel as packed bed substances was surveyed by Ramadan et al. (2007). In their study, it was concluded that thermal efficiency of DPSAHPB is enhanced with lower porosity and higher mass flow.

In another experimental research, Sopian et al. (2009) proposed the double pass SAH having porous media in the lower channel. Their results showed that the thermal performance of SAH is improved by adding the porous materials in the second channel of the double pass SAH. Prasad et al. (2009) surveyed on heat transfer and friction characteristics of packed bed SAH which utilized wire mesh as packing material. Their finding revealed that heat transfer coefficient enhances by increase of mass flow rate and reduction in porosity. Aldabbagh et al. (2010) presented analysis of thermal

performances for single and double pass SAHs with steel wire mesh layers and common collectors at different mass flow rates. They indicated that double pass SAHs with wire mesh have higher thermal efficiency than regular SAHs. The influence on the performance of utilizing porous material in double pass SAH is investigated by Ramani et al. (2010). Their effort revealed that thermal performance of double pass SAH having porous material is better than the SAH without porous material and single pass SAH by 25% and 35% respectively.

In 2010, Omojaro and Aldabbagh indicated that SAHs, single or double pass, which utilized steel wire mesh layers and also fins to reach higher efficiency than regular ones. Their investigation illustrated that thermal efficiency is increased by use of double pass SAH having steel wire mesh arranged in layers as an absorber plate and packing material. The packed bed SAH using blackened wire mesh screen matrices is proposed by Lalji et al. (2011). They obtained that the thermal performance of packed bed SAH is enhanced by lower porosity. An experimental investigation on single pass SAH with various porous media is accomplished by Kapardar and Sharma (2012) which showed that SAH with steel wool has better efficiency than single pass SAH having glass wool. Fudholi et al. (2013) evaluated thermal performance of double pass SAH with and without fins and also they reported that efficiency increases by using fins on absorber plate. Recently, a scientific study was conducted on heat transfer and thermal performance of SAH with longitudinal fins by Chabane et al. (2013). Their efforts showed that the highest thermal efficiency and maximum increase of outlet temperature were obtained by the finned SAH. Thermal performance of wire mesh packed double pass SAHs with external

recycle is analyzed by Chii-Dong Ho et al. (2013) and their results demonstrated significant improvement in heat transfer.

Singh and Dhiman (2014) proposed analytical models to estimate the thermal and thermohydraulic efficiencies of two configurations of double pass packed bed SAH under external recycle. Nowzari et al. (2014) investigated the thermal performances of single and double pass SAHs having regular glazing and also with quarter perforated cover. It is concluded that thermal efficiency of SAH with 10D perforated cover is greater than SAH with 20D perforated cover. Mahmood et al. (2015) utilized several mesh layers and also transverse fins for single and double pass SAHs to obtain high thermal performance. Furthermore, thermal performance of double pass SAH having wire mesh is compared with other configurations of SAHs by Chii-Dong Ho et al. (2015). Anandh and Baskar (2015) evaluated performance of double pass SAH with porous materials and also they demonstrated that double pass SAH with steel wool as porous material has higher thermal performance than conventional SAH. Denga et al. (2015) illustrated that thermal performance of SAH is increased by cleaning glass cover of a SAH. A literature review demonstrated that there is no experimental study on utilizing perforated glass as a cover of SAH to reduce heat loss and also lack of attempt to adjust SAH with the appearance of buildings. The main purpose of the current study is to survey the thermal performance of different configurations of PGSAHs and compare them with the UTSAH by means of series of experiments which are carried out in the same environment.

Chapter 3

EXPERIMENTAL SETUP

Among the literature, there are tremendous investigations on modifications of SAHs and scholars proposed several ways to increase the thermal efficiency and decrease the heat loss from SAHs. In the present study, the new type of SAH is presented which is called PGSAH as demonstrated in Figure 6 with perforated plexi glass as a glazing of the SAH. The study is divided into two parts which contains two series of experiments on PGSAHs. The first series of experiments are conducted on coloured PGSAHs and a black UTSAH at different mass flow rates. The second series of experiments has accomplished on two DPGSAHPBs and a UTSAH.

3.1 Coloured PGSAHs and UTSAH

In first series of experiments, the thermal performances of SPGSAHs having different inner collector colours and a black coloured UTSAH are studied experimentally (Figure 7). Moreover, two SPGSAHs having perforated plexiglas glazing with different inner colours were constructed. The third SAH is a UTSAH where the top cover was black coloured perforated sheet metal. The three SAHs are tested simultaneously at same mass flow rates.

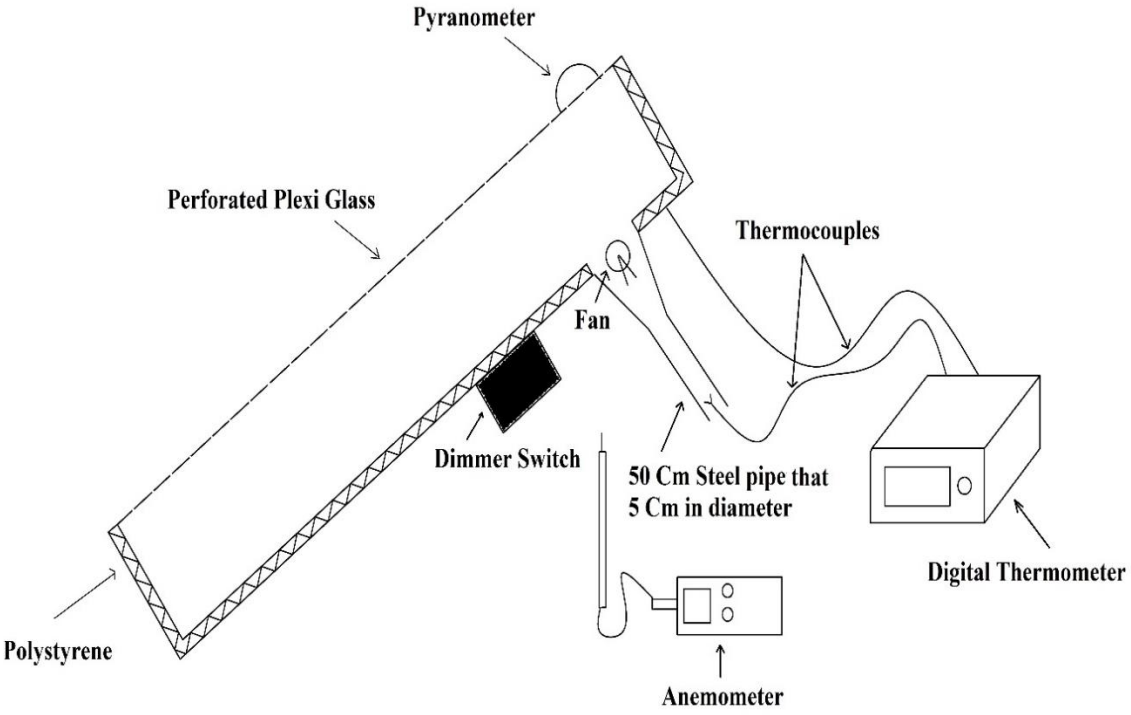

Figure 6: Schematic of PGSAH.


Figure 7: Two Different PGSAHs & UTSAH Simultaneously.

The two SPGSAHs and a black UTSAH experimentally were tested in the city of North Cyprus, Famagusta. Moreover, experiments were conducted on SAHs in clear days of December and November of 2012.

3.1.1 Experimental Setup and Proceedings

All SAHs are made of wood and have same aperture area of $0.81 m^2$ with 0.9 m width and 0.9 m length. The size of these collectors are smaller than conventional SAHs for practical reasons. The Plexi glass cover, as glazing part of SPGSAH, is situated on top of the collector which has 3 mm thickness and 3 mm diameter holes and dimensions of (88× 88) cm^2 (Figure 8). Moreover, the centre to centre distance between holes of perforated Plexiglas (pitch) were 3 cm (Figure 8). The black perforated sheet metal cover of UTSAH was drilled as same as perforated plexi glass. The distance between covers and bottom of SAHs which creates plenum were 30 cm.

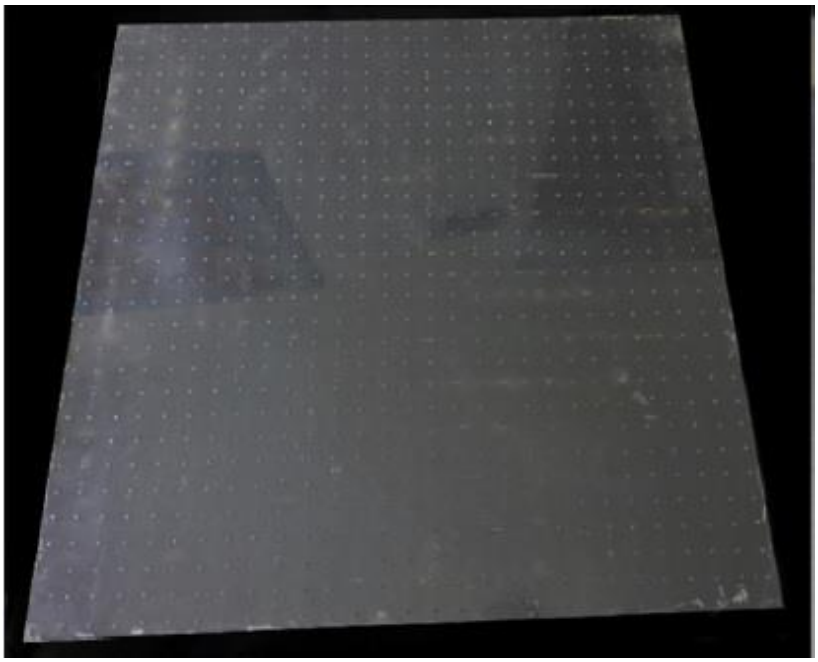

Figure 8: Perforated Plexi Glass

The blue, red, green, light yellow, violet and white colours are used for inside of collectors. The radial fans 600 W were situated underneath of box (Figure 9). The fan sucks heated air into collector via holes of perforated plexi glass by creation of airflow and negative pressure inside SAH (Figure 9). The air flow rate is controlled by the use of dimmer switches.

Figure 9: Radial Fan

In order to decrease heat loss from SAHs, the side and bottom of collectors were insulated by 30 mm polystyrene. A 50 cm pipe has been installed on the outlet of SAH in order to achieve fully developed flow. The speed of air was determined by use of Extech 407112 Vane Anemometer with reading accuracy of ± (2% + 0.2 m/s) (Figure 10).

Figure 10: The Extech 407112 Vane Anemometer

Inlet and outlet air temperatures (T_{in} and T_{out}) were determined by using T-type thermocouples (Figure 11). A thermocouple was situated inside the 50 cm pipe to measure T_{out}. Two thermocouples were located underneath of box to determine temperature of ambient air (T_a).


Figure 11: T-type thermocouple

Figure 12: Ten-channel Digital Thermometer

Furthermore, T_{in}, T_{out} and T_a were recorded by Ten-channel Digital Thermometer with the model of Omega MDSSi8 Series digital which has accuracy of $\pm 0.5℃$ (Figure 12).

The amount of solar radiation on surface of SAH is determined by an Eppley Radiometer Pyranometer (PSP) with accuracy between (-0.5,+0.5) % between range of 0 and $2800\,\frac{W}{m^2}$. In addition, the PSP is placed on the top of SAHs (Figure 13).


Figure 13: Eppley Radiometer Pyranometer

On the basis of geographical place of Cyprus (33.95°E, 35.125°N), SAHs were situated toward south and collectors are tilted 36° with regard to horizontal axis to harness highest amount of solar radiation incident on the cover of collector (Tiwari, 2002). During experiments T_{in}, T_{out}, T_a, solar intensity and mass flow rates were recorded every half an hour from 9 am to 3 pm.

3.2 DPGSAHPBs and UTSAH

In second section of experiments, thermal performance of DPGSAHPB is investigated. Two different configurations of DPGSAHPBs and black UTSAH are tested simultaneously. DPGSAHPBs is constructed in order to decrease heat losses from cover and substantial enhancement of thermal efficiency was obtained. The DPGSAHPB consists of perforated plexi glass as a glazed cover and a glass inside the collector, air blower and mesh layers or iron wools are used as packed bed. Moreover, mesh layers or iron wools were utilized as an absorber which are not expensive and also they are painted in black to increase absorptivity. In fact, the surface area per unit volume ratio is increased by utilization of packing material which could enhance efficiency of a collector.

Experimental set up includes the arrangement of two DPGSAHs with packed bed and unglazed transpired solar air heater (UTSAH) with same size (Figure 14). The schematic diagrams of the constructed DPGSAHPBs and UTSAH are shown in Figure 15. The series of experiments were done in the days of July and August 2013 under climatic conditions of Famagusta city, Cyprus.

Figure 14: DPGSAHPB with mesh layers, DPGSAHPB with iron wools and transpired SAH

3.2.1 Experimental Setup and Proceedings

Due to practical reasons the size of these apparatuses are smaller than that of conventional SAHs which the length and width of the collectors were taken as 90 cm×90 cm respectively.

The body of SAH was insulated by 3 cm thick polystyrene externally and blackened internally to minimize the heat losses.

DPGSAHPB consists of perforated plexi glass (PPG), normal glass, several steel wire mesh layers or iron wools, radial fan without absorber plate (Figure 16). The dimensions of PPG are (88×88) cm^2 and the diameter of holes in PPG is 3 mm with the pitch (distance between holes) of 3 cm. Normal window glass with 3 mm thick, dimensions of (85×60) cm^2, which is situated inside the DPGSAHPB at the 10 cm from PPG. For the first DPGSAHPB, nineteen blackened steel wire mesh layers, (1.2×1.2) cm^2 in cross section voids and 0.085 cm in diameter of wire, were packed parallel between upper side of normal glass and back of perforated plexi glass. Moreover, the distance between each

mesh layer was 0.5 cm. For second DPGSAHPB, 60 blacked iron wools were fixed between upper side of the normal glass and back side of perforated plexi glass. The porosity of mesh layers and iron wools inside both DPGSAHPBs is equal to 98.3%. UTSAH comprises of blacked perforated metal sheet as a cover of collector which holes' diameter are 3 mm and the space between holes is 6 cm without any packing material. The air flow inside the SAH was circulated by the radial fan with a 120 W power that was located at the backside of collector. The experiments were performed under various mass flow rates. As in the first section, the air velocity was measured by the use of Vane Anemometer and also values of mass flow rates were adjusted by dimmer to keep constant.

Moreover, the solar radiation incident on a collector was obtained by means of a Pyranometer which was located on the cover of collector. Moreover, SAHs were placed southward at an angle of 36^{o} with respect to the horizontal. The temperatures were obtained by T-type thermocouples and also ten-channel digital thermometer was used to record all of the temperature data. The air was circulated daily for 7 hours of the days at different mass flow rates. Additionally, measurements of $T_{in,}$ T_{out}, T_a and solar intensity for all apparatuses were recorded every 30 min prior to the period at the same mass flow rate simultaneously.

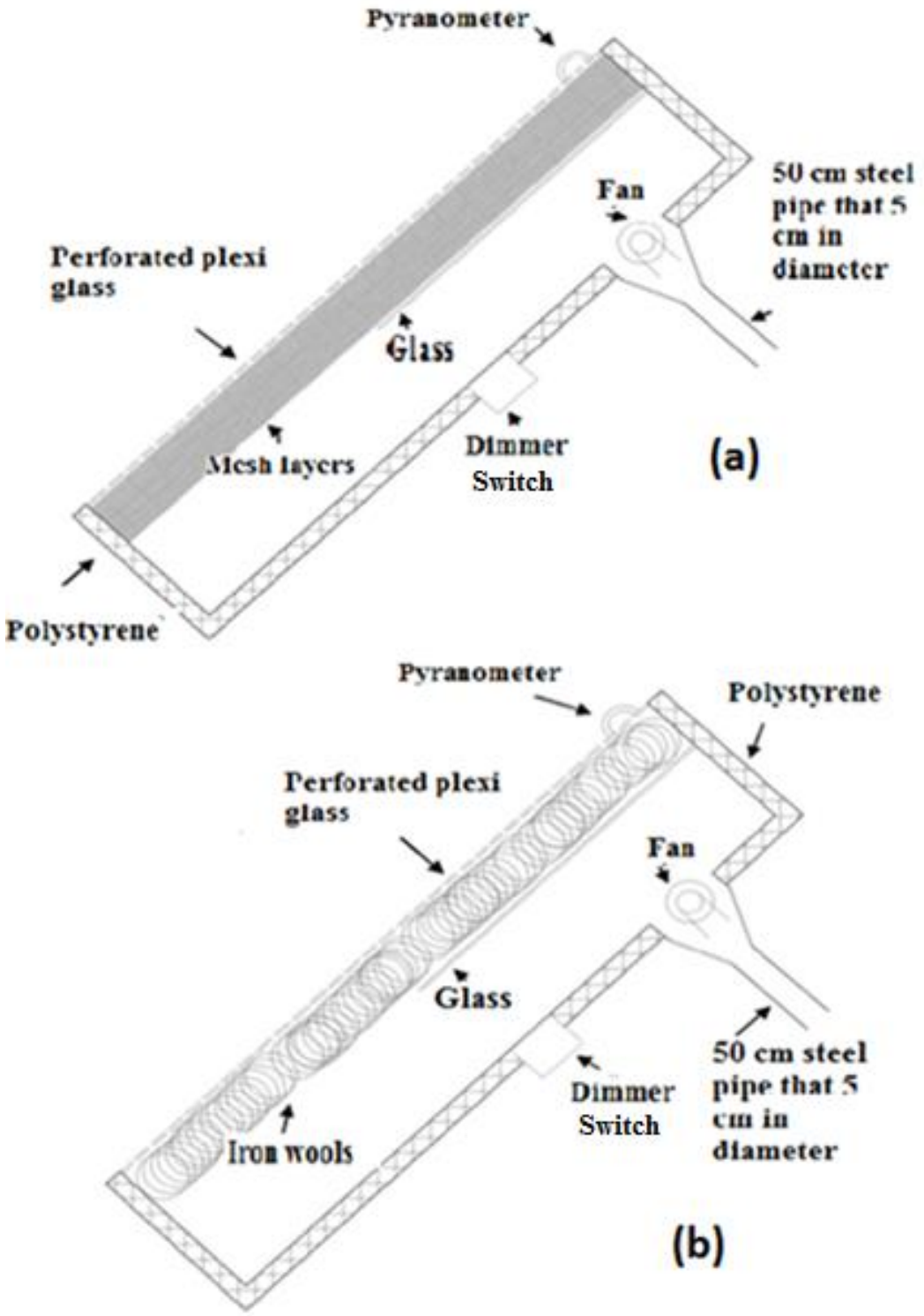

Figure 15: Schematic of (a) DPGSAHPB with mesh layers, (b) DPGSAHPB with iron wool

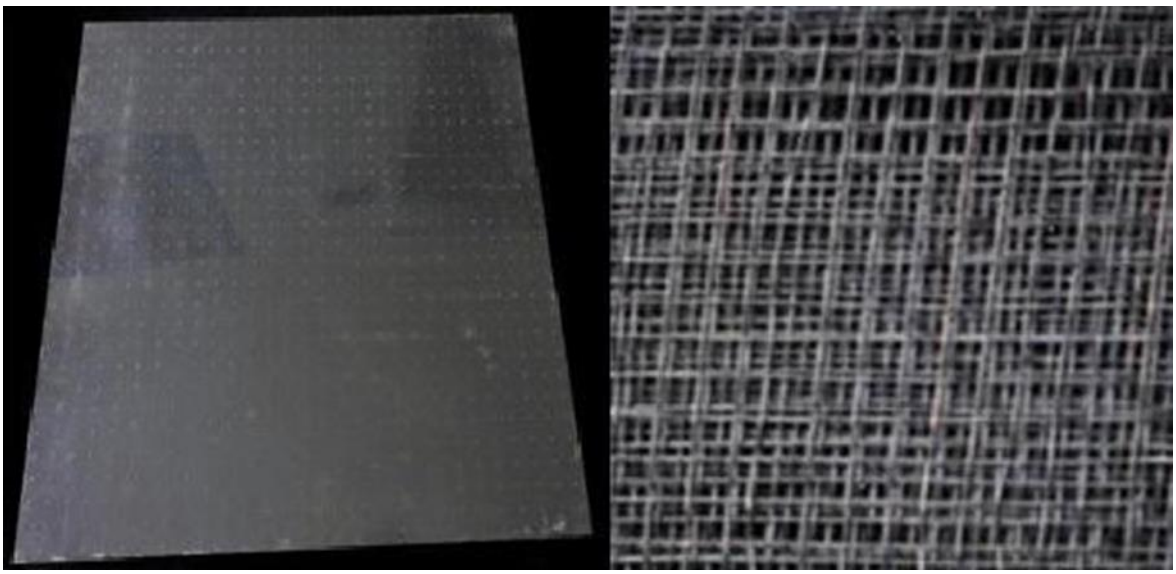

(a) **(b)**

(c)

Figure 16: (a) Perforated plexiglas cover of DPGSAHPB. (b) Steel wire mesh layers (c) Iron wools

Chapter 4

MATHEMATICAL MODEL

Figures 17 and 18, show schematic diagrams of different types of perforated glazed solar air hearts utilized in current survey. A mathematical model for different type of perforated glass SAH below forced convection position is illustrated. In addition, the analysis is on the basis of analytical solutions for the energy balance of various parts of specified systems.

The energy balance equations for each component of SAH are proposed under specific assumptions:

1) The experiments test under steady state situations.

2) The heat capacities of plexiglas, normal glass and insulation are insignificant.

3) There is only one dimensional flow and the variations of air temperature is along the direction of flow.

4) Thermo physical properties of flowing air are varied with temperature linearly.

5) There is no temperature difference among the thickness of the plexi glass and normal glass.

6) Temperature of sky is similar to temperature of ambient air.

Based on mentioned assumption, the energy balance equations for different parts of coloured SPGSAH is written as follows:

(a) Perforated plexi glass:

$$I.\propto_g = h_w(T_g - T_a) + h_{rga}(T_g - T_a) + h_{cgf}(T_g - T_f) + h_{rgb}(T_g - T_b) \quad (5)$$

Where I is intensity, $\propto_g$ is absorptivity of PPG, h_w is heat transfer coefficient of wind, T_g is temperature of PPG, T_a is ambient temperature, h_{rga} is radiative heat transfer coefficient between PPG and air, h_{cgf} is convective heat transfer coefficient between PPG and fluid (air flows inside collector), T_f is temperature of fluid, h_{rgb} is radiative heat transfer coefficient between PPG and back of collector, T_b is temperature of back.

(b) Bottom of collector:

$$h_{rbg}(T_g - T_b) = h_{cbf}(T_b - T_f) + U_b(T_b - T_a) \quad (6)$$

(c) Air flowing:

$$M_f . C_f \frac{\partial T_f}{\partial t} + G\frac{C_f}{w}\frac{\partial T_f}{\partial x} = h_{cbf}(T_b - T_f) + h_{cgf}(T_g - T_f) \quad (7)$$

Where h_{cbf} is convective heat transfer coefficient between back and fluid, U_b is back loss coefficient, M_f is mass of fluid, C_f is specific heat transfer of fluid, G is mass velocity and w is width of the collector.

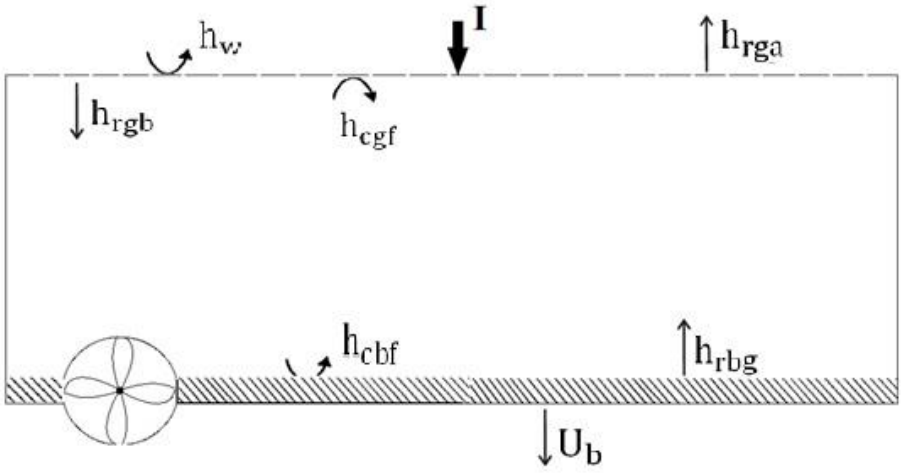

Figure 17: Schematic view of the energy balance of coloured SPGSAHs

The energy balance equations for different parts of the DPGSAHPB is written as:

a) Perforated plexi glass:

$$I.\propto_{g1}=(h_{rg1a}+h_w)(T_{g1}-T_a)+h_{rg1m}(T_{g1}-T_m)+h_{cg1f1}(T_{g1}-T_{f1}) \quad (8)$$

Where $\propto_{g1}$ is absorptivity of PPG, h_{rg1a} is radiative heat transfer coefficient between PPG and ambient air, T_{g1} is temperature of PPG, h_{rg1m} is radiative heat transfer coefficient between mesh layers and PPG, T_m is temperature of mesh layers, h_{cg1fl} is convective heat transfer coefficient between PPG and air flows in first passage.

b) Packing material:

$$I.\propto_m.\tau_{g1}=h_{rg1m}(T_m-T_{g1})+h_{rmg2}(T_m-T_{g2})+h_{cmf1}(T_m-T_{f1}) \quad (9)$$

Where $\propto_m$ is absorptivity of mesh layers, τ_{g1} is transmissivity of PPG, h_{rmg2} is radiative heat transfer coefficient between mesh layers and inner glass, T_{g2} is temperature of inner glass, h_{cmfl} is convective heat transfer coefficient between mesh layers and air flows in first passage, T_{fl} is temperature of air flows in first passage.

c) Normal glass inside the collector:

$$I.\alpha_{g2}.\tau_{g1}.\tau_{g2}=h_{rg2m}(T_{g2}-T_m)+h_{cg2f1}(T_{g2}-T_{f1})+h_{cg2f2}(T_{g2}-T_{f2})+h_{rg2b}(T_{g2}-T_b) \quad (10)$$

Where α_{g2} is absorptivity of inner glass, τ_{g2} is transmissivity of inner glass, h_{cg2fl} is convective heat transfer coefficient between inner glass and air flows in first passage, h_{cg2f2} is convective heat transfer coefficient between inner glass and air flows in second passage, T_{f2} is temperature of air flows in second passage, h_{rg2b} is radiative heat transfer coefficient between back and inner glass.

d) Air flowing between plexi glass, packing materials and normal glass:

$$\frac{\dot{m}_{f1}.C_{g2}}{w}.\frac{\partial T_{f1}}{\partial x}=k_m.\frac{\partial^2 T_{f1}}{\partial x^2}+h_{cg1f1}(T_{g1}-T_{f1})+h_{cmf1}(T_m-T_{f1})+h_{cg2f1}(T_{g2}-T_{f1}) \quad (11)$$

Where C_{g2} is specific heat transfer of inner glass, k_m is thermal conductivity of mesh layers, h_{cbf2} is convective heat transfer coefficient between back and air flows in second passage, $\dot{m}_{f1}$ is mass flow rate of air flows in first passage, $\dot{m}_{f2}$ is mass flow rate of air flows in second passage.

e) Bottom of collector:

$$h_{rg2b}(T_{g2}-T_b)=h_{cbf2}(T_b-T_{f2})+U_b(T_b-T_a) \quad (12)$$

f) Air flowing flow between normal glass and bottom of collector:

$$\frac{\dot{m}_{f2}.C_{g2}}{w}.\frac{\partial T_{f2}}{dx}=h_{cg2f2}(T_{g2}-T_{f2})+h_{cbf2}(T_b-T_{f2}) \quad (13)$$

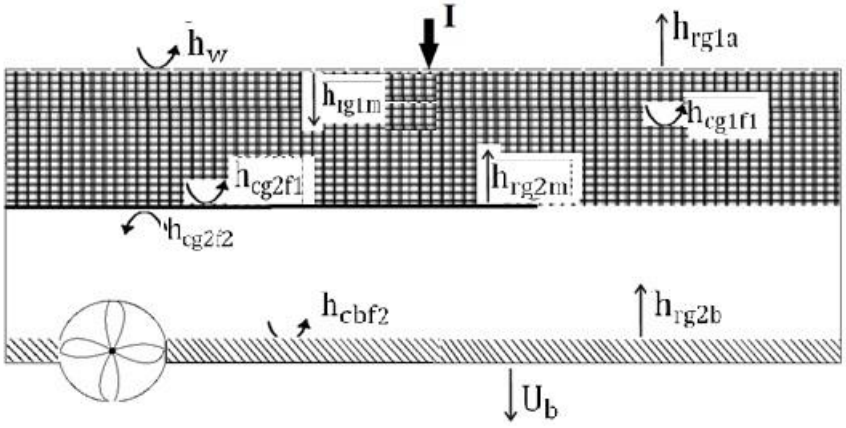

Figure 18. Schematic view of the energy balance of DPGSAHPB

The heat transfer coefficients of the various parts of the SAHs are measured by using following correlation as:

$$h_{rg1a}=\frac{\partial(T_{g1}^2+T_a^2).(T_{g1}+T_a)}{\left[\frac{1}{\varepsilon_{g1}}-1\right]} \quad (14)$$

$$h_{rg2m}=\frac{\partial(T_{g2}^2+T_m^2).(T_{g2}+T_m)}{\left[\frac{1}{\varepsilon_{g2}}+\frac{1}{\varepsilon_m}-1\right]} \quad (15)$$

$$h_{rg2b} = \frac{\partial(T_{g2}^2+T_b^2).(T_{g2}+T_b)}{\left[\frac{1}{\varepsilon_{g2}}+\frac{1}{\varepsilon_b}-1\right]} \quad (16)$$

In addition, the convective heat transfer coefficient of air flowing on surface of perforated plexi glass is measured by following formula which is proposed by McAdam (1954):

$$h_w = 5.7 + 3.8V \quad (17)$$

Mittal and Varshney (2006) stated that for packing materials, heat transfer coefficient h_{cmfu} is measured by formulas which j_H factor is depended to Stanton number and calculates as follows:

$$j_H = St_m.(pr)^{2/3} = 0.647\left[\frac{1}{n\varphi}.\left(\frac{P_t}{d_w}\right)\right]^{2.104} Re_m^{-0.55} \quad (18)$$

which Stanton number is determined by

$$St_m = \frac{h_{cmf1}}{G_0 C_p} \quad (19)$$

The convective heat transfer between the air flowing in packing materials and glass, h_{cgf1} is calculated as

$$h_{cgf1} = \frac{Nu_m K_f}{\varphi D_{h1}} \quad (20)$$

where D_{h1} is defined as hydraulic diameter of collector which is calculated as

$$D_{h1} = \frac{4A_{f1}}{p} = \frac{2(wd_1)}{(w+d_1)} \quad (21)$$

Nu_m is the Nusselt number of packing materials which is obtained by

$$Nu_m = 0.2Re_m^{0.8}Pr^{1l3} \quad (22)$$

where, $Re_m$is Reynolds's number for packing materials and is given

as Thakur et al., (2003).

$$Re_m = \frac{4r_H G_0}{\mu} \quad (23)$$

$$r_H = \frac{\varphi d_w}{4(1-\varphi)} \tag{24}$$

r_H is Hydraulic radius which is referred to the size of packing and the void space. G_0 is the mass velocity, kg/sm^2 is given by

$$G_0 = \dot{m}/(A_c)\varphi \tag{25}$$

φ is the porosity of the mesh layers as packed bed which is obtained as follows (Thakur et al., 2003) (Figure 19) :

$$\varphi = \frac{P_t^2 d - \left[\frac{\pi}{2}(d_w)^2 P_t\right] n}{P_t^2 d} \tag{26}$$

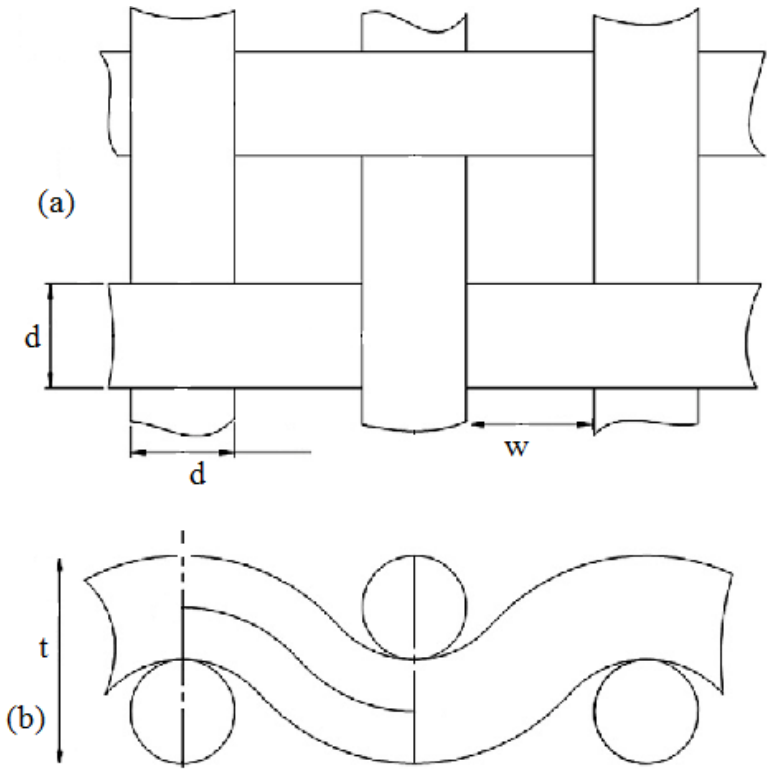

Figure 19: Schematic of wire mesh layer (a) Top view (b) Front view (Zenghui Zhao et al., 2013)

For turbulent flow (Re > 6000) Nusselt number is obtained by

$$\mathrm{Nu} = 0.018\mathrm{Re}^{0.8}\mathrm{Pr}^{0.4} \quad (27)$$

The convective heat transfer coefficient for the air flowing between normal glass and bottom of collector as follows

$$\mathrm{h_{cbf2}} = \mathrm{Nuk/D_{h2}} \quad (28)$$

The main design parameters which are utilized are as follows:

width of collector, w = 0.9 m

length of collector, L= 0.9 m

depth of upper part of collector: 0.15 m

depth of lower part of collector: 0.15 m

transmissivity of the glass covers, $\tau_g = 0.9$

absorptivity of the plexi glass, $\alpha_g = 0.05$

absorptivity of packing materials, $\alpha_g = 0.95$

conductivity of packing materials, $k_m = 45$ W/M.K

Chapter 5

RESULTS AND DISCUSSION

This experimental study includes two series of experiments which are investigated on novel SAH so called perforated glazed solar air heater (PGSAH). The first series of experiments contains the analysis of thermal performance of coloured SPGSAHs and black UTSAH. In second section of experiments, thermal performance of DPGSAHPBs is evaluated and also thermal performance of UTSAH is compared with them. The main purpose of this investigation is to open new horizon in context of solar air heating to enhance thermal efficiency and reduce heat loss and also finding proper integration SAHs and facade of building.

5.1 Analysis of Thermal Performance of Coloured SPGSAHs

The thermal performances of coloured SPGSAHs and UTSAH were investigated experimentally between 12.11.2012 and 31.12.2012, under weather of Famagusta the city of North Cyprus. During this study, the average value of wind speed was 5.34 m/s. Three solar air heaters were tested simultaneously which included two coloured SPGSAHs and a UTSAH. Figure 20 shows trend of solar intensity versus standard local time during a day where maximum value of solar intensity was obtained at noon time. The maximum value of solar radiation intensity was 914.2857 W/m^2 at 12:30 and the average intensity was 756.71 W/m^2.

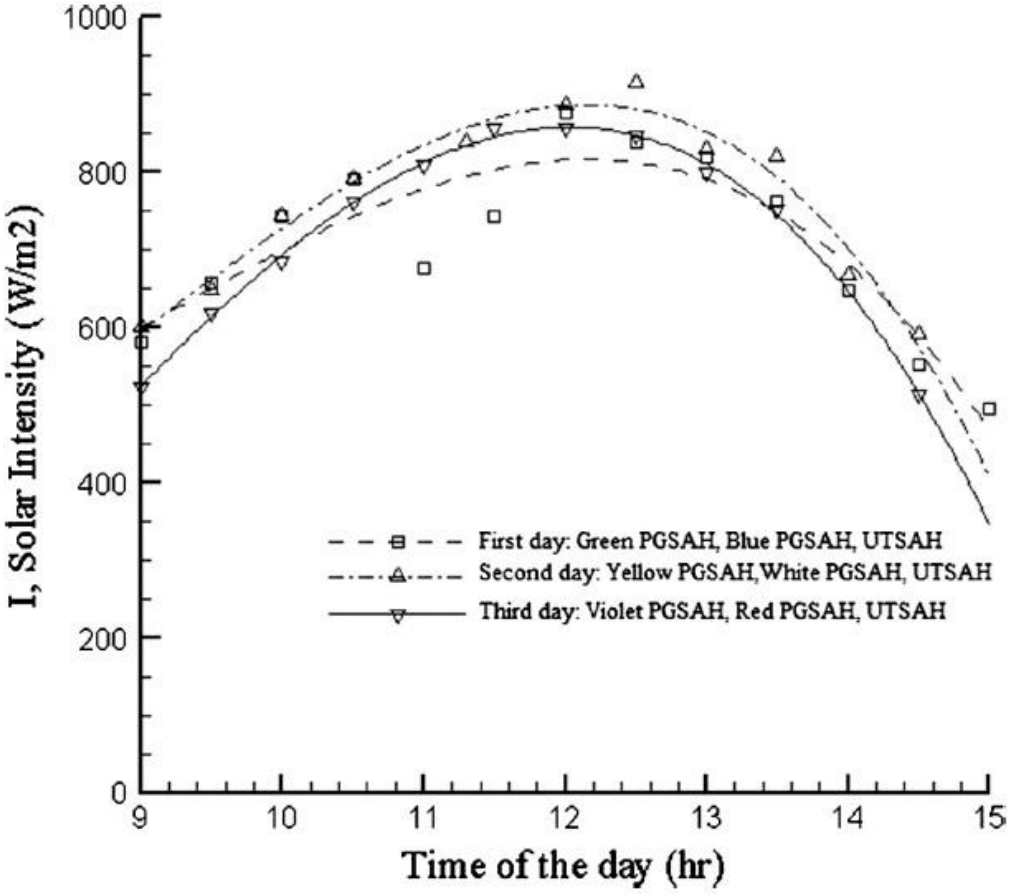

Figure 20: Solar intensity versus different standard local time of days for different SPGSAH's and UTSAH on three different days.

The performances of SPGSAHs having different inner collector colours were investigated between the range of air mass flow rate 0.017 and 0.036 kg/s. Figures 21-26, show the variations of temperature differences ($\Delta T = T_{out} - T_{in}$) versus time of day for coloured SPGSAHs and UTSAH at $\dot{m} = 0.036$ kg/s and $\dot{m} = 0.024$ kg/s. The diagrams illustrated that ΔT reduces with higher mass flow rates. Moreover, ΔT increases to maximum at noon time and then ΔT decreases during the afternoon.

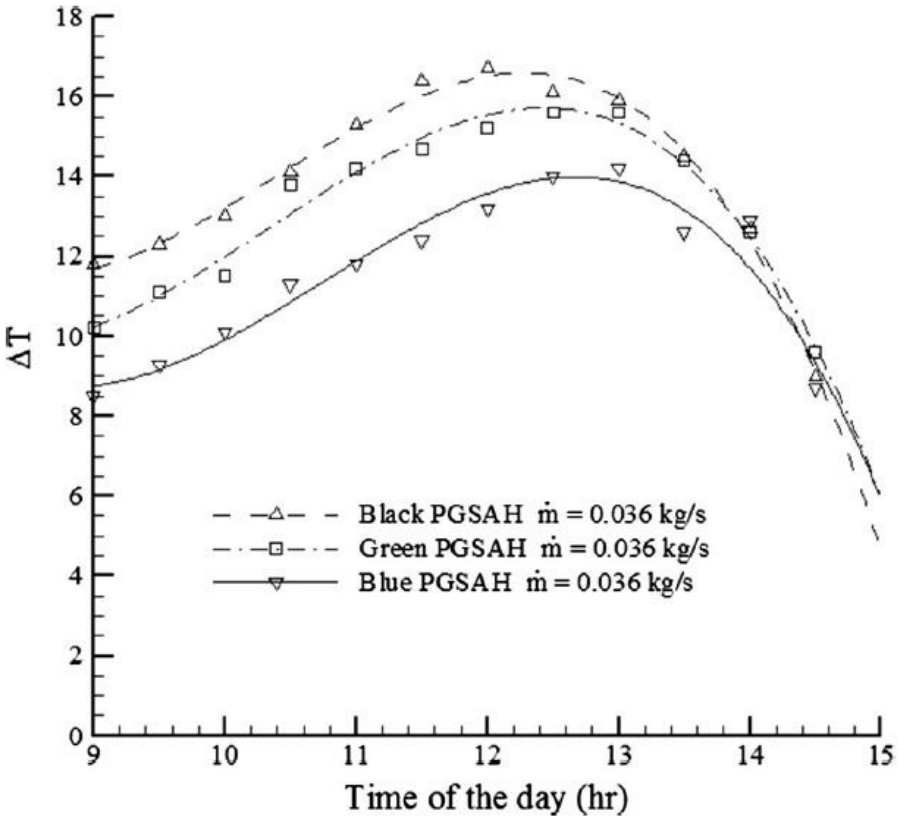

Figure 21: Variations of exit and inlet air temperature difference versus time of the dayfor black PGSAH, green PGSAH and blue PGSAH for ṁ = 0.036 kg/s.

For black, green and blue PGSAHs, at the mass flow rate of 0.024 kg/s, the maximum values of ΔTs were 17.9 ℃, 17.3℃ and 15.4℃ at 13:00 h (Figure 24). The results indicated that black PGSAH creates the highest ΔT and also green, blue and red produced higher ΔT compared with light coloured PGSAHs. The minimum ΔT is obtained by yellow PGSAH which was 9.4℃ at mass flow rate of 0.036 kg/s at 13:00 h. For UTSAH, the lowest temperature difference was 9.2℃ at mass flow rate of 0.036 kg/s at 13:00 h (Figure 23).

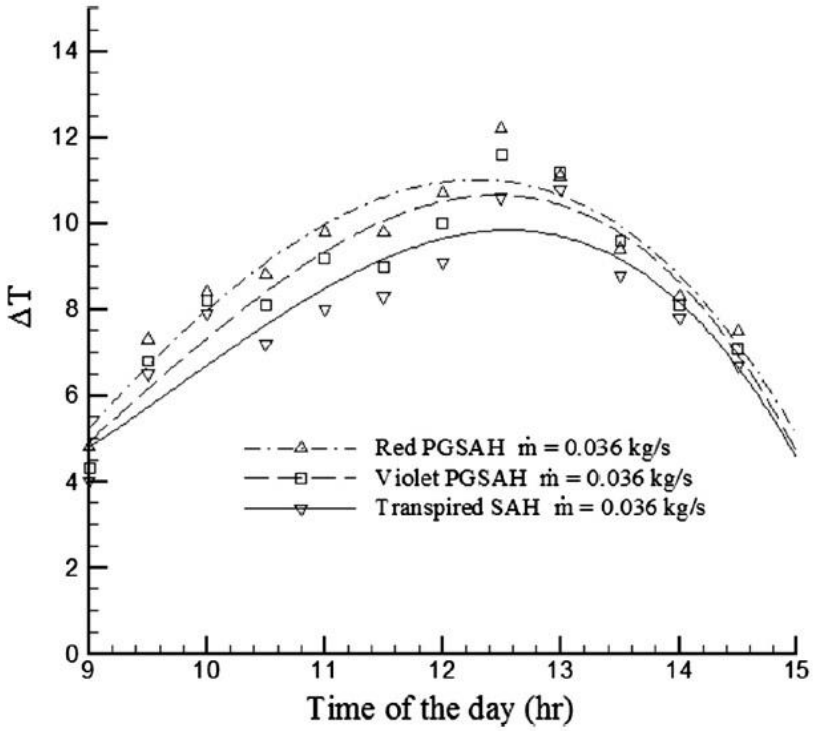

Figure 22: Variations of exit and inlet air temperature difference versus time of the dayfor red PGSAH, violet PGSAH and UTSAH for ṁ = 0.036 kg/s.

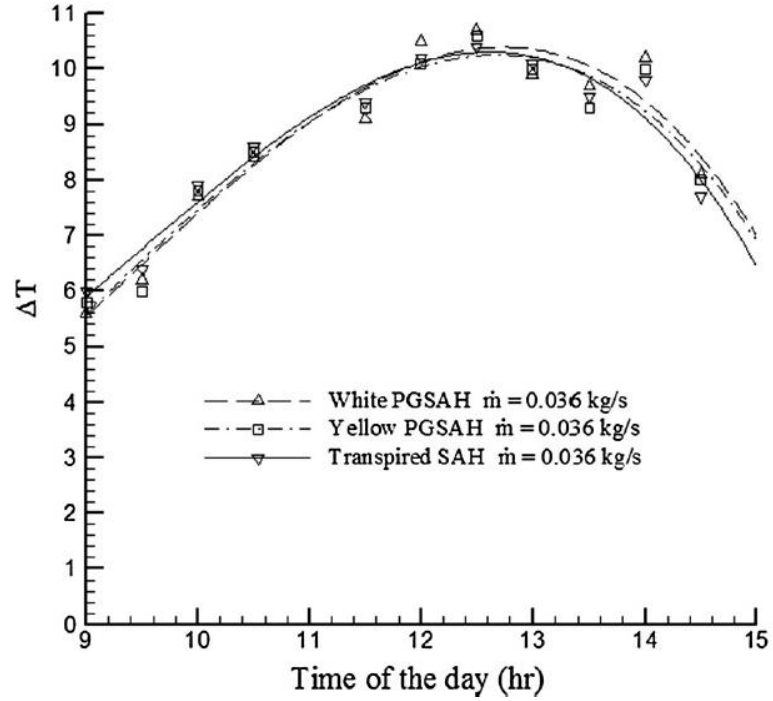

Figure 23: Variations of exit and inlet air temperature difference versus time of the day for white PGSAH, yellow PGSAH and UTSAH for ṁ = 0.036 kg/s.

Figures 21, 22, 24 and 25 illustrated that dark coloured SPGSAHs obtain higher ΔT than UTSAH ones. Moreover, the ΔTs which is created by white or light yellow coloured PGSAHs has similar value with ΔT of UTSAH's (Figures 23 and 26).

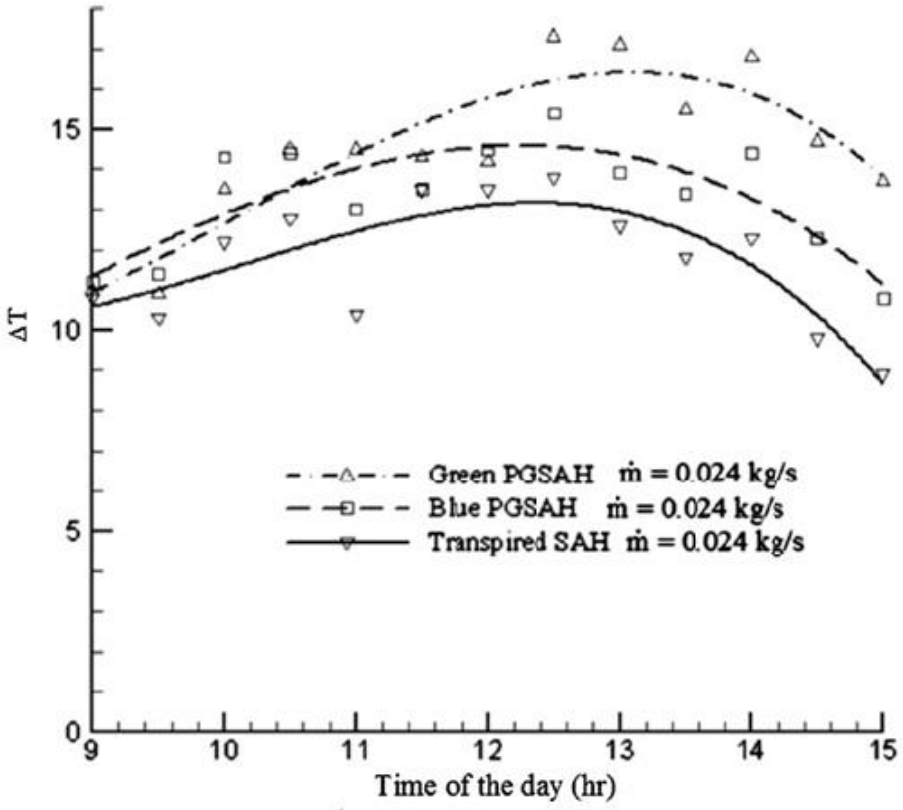

Figure 24: Variations of exit and inlet air temperature difference versus time of the day for blue PGSAH, green PGSAH and UTSAH for ṁ = 0.024 kg/s.

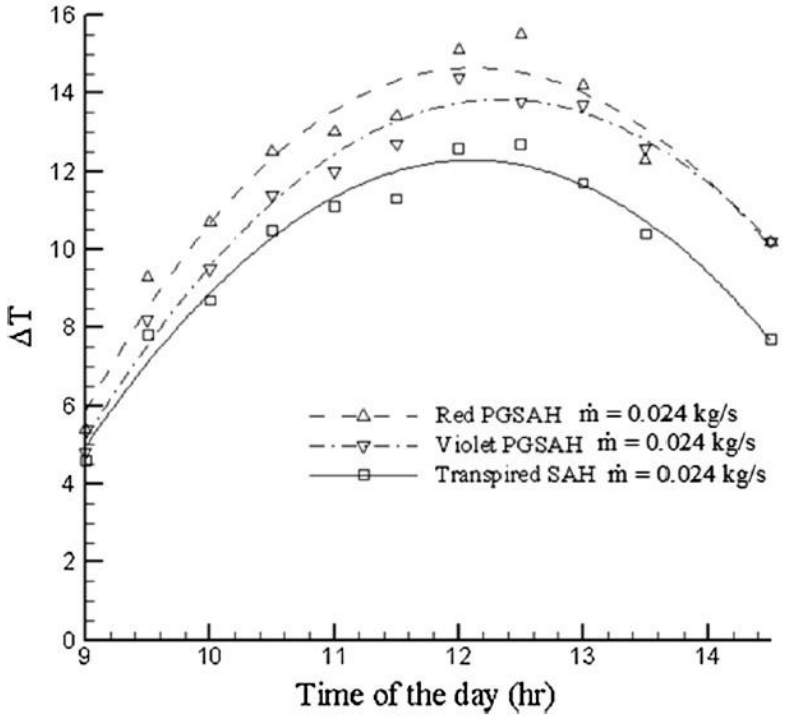

Figure 25: Variations of exit and inlet air temperature difference versus time of the day for red PGSAH, violet PGSAH and UTSAH for ṁ = 0.024 kg/s.

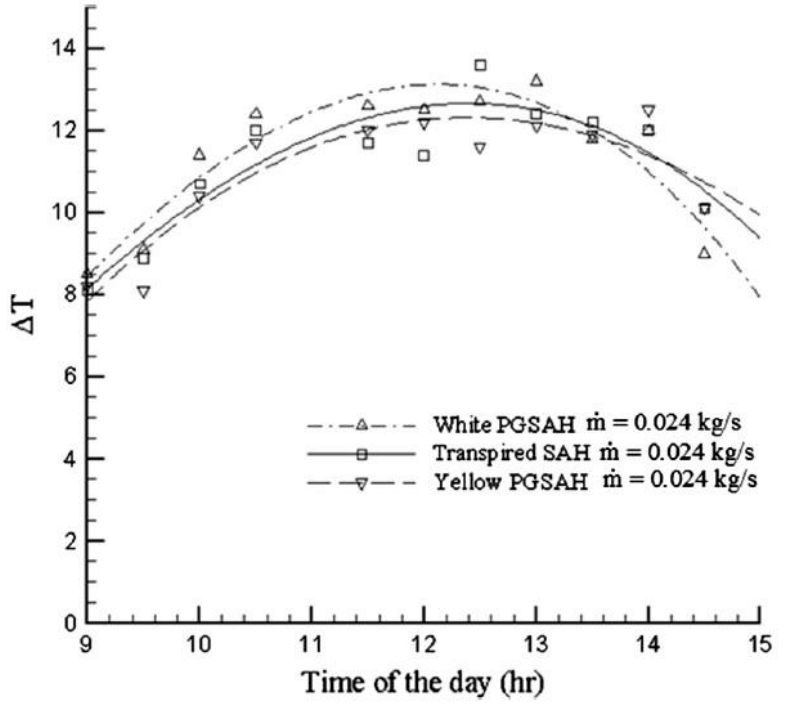

Figure 26: Variations of exit and air temperature difference versus time of the day for white PGSAH, yellow PGSAH and UTSAH for ṁ = 0.024 kg/s.

Figures 27-32, illustrate the efficiency versus standard local time of the day for different coloured PGSAHs and UTSAH at mass flow rates of 0.036 kg/s and 0.024 kg/s.

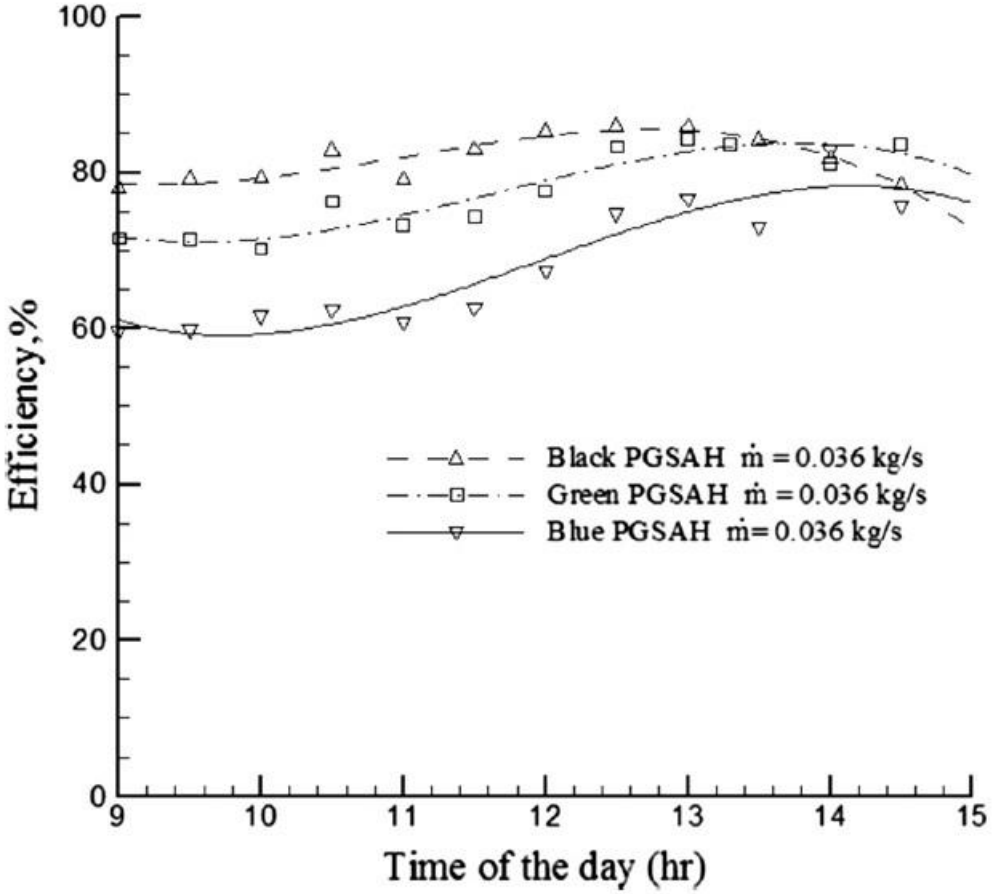

Figure 27: Thermal efficiency of black PGSAH, green PGSAH and blue SAH versus time of the day for ṁ = 0.036 kg/s.

Figure 27 demonstrates maximum values of thermal efficiency for black, green, blue PGSAHs which are 85%, 84% and 76% respectively at mass flow rate of 0.036 kg/s. Moreover, results illustrated thermal efficiency of coloured PGSAH enhances from 9 am to 15 pm. Furthermore, the thermal efficiency increases as air mass flow rates increased.

The thermal efficiency of black, green and blue PGSAHs are higher than the light coloured PGSAH and UTSAH for the same mass flow rate (Figures 27-32).

Figure 28 illustrates that highest values of thermal efficiency for red and violet coloured PGSAHs were 65%, 61% respectively at mass flow rate of 0.036 kg/s.

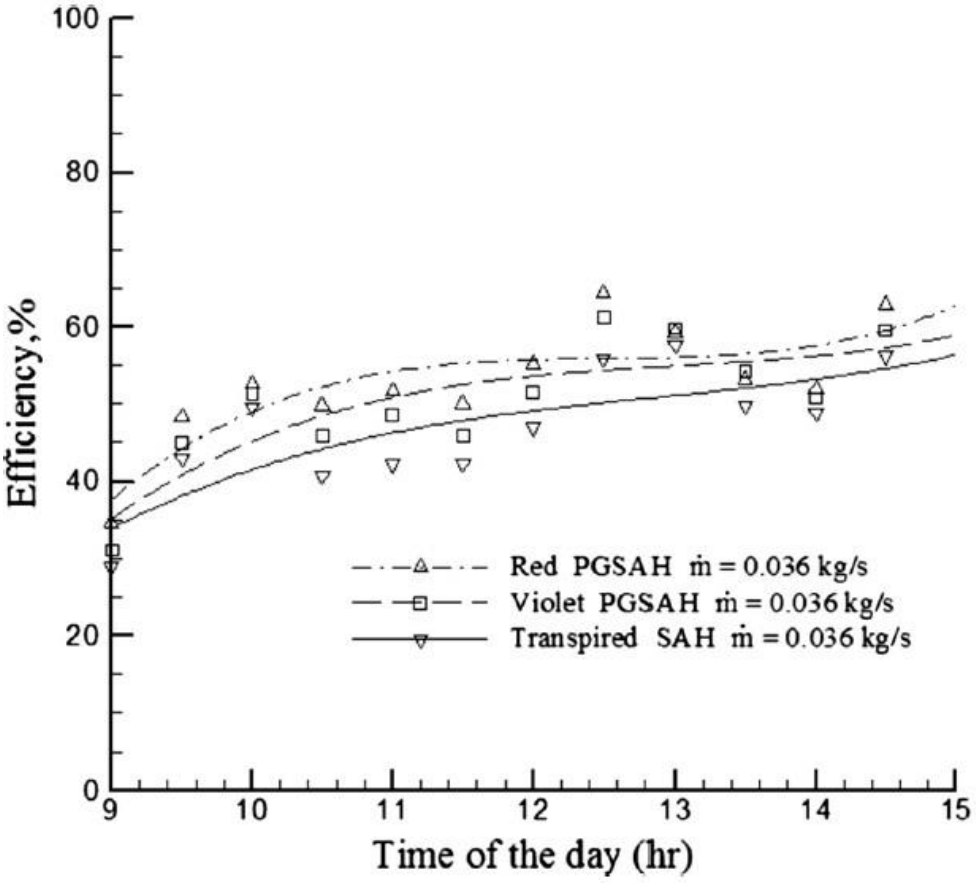

Figure 28: Efficiency of red PGSAH, violet PGSAH and UTSAH versus time of the day for ṁ = 0.036 kg/s.

Figure 29 shows that the highest values of thermal efficiencies for light yellow, white PGSAHs and UTSAH were 54%, 52% and 55% at noon time respectively at the mass flow rate of 0.036 kg/s. As diagram demonstrates that thermal efficiency of light colour PGSAH is similar to UTSAH.

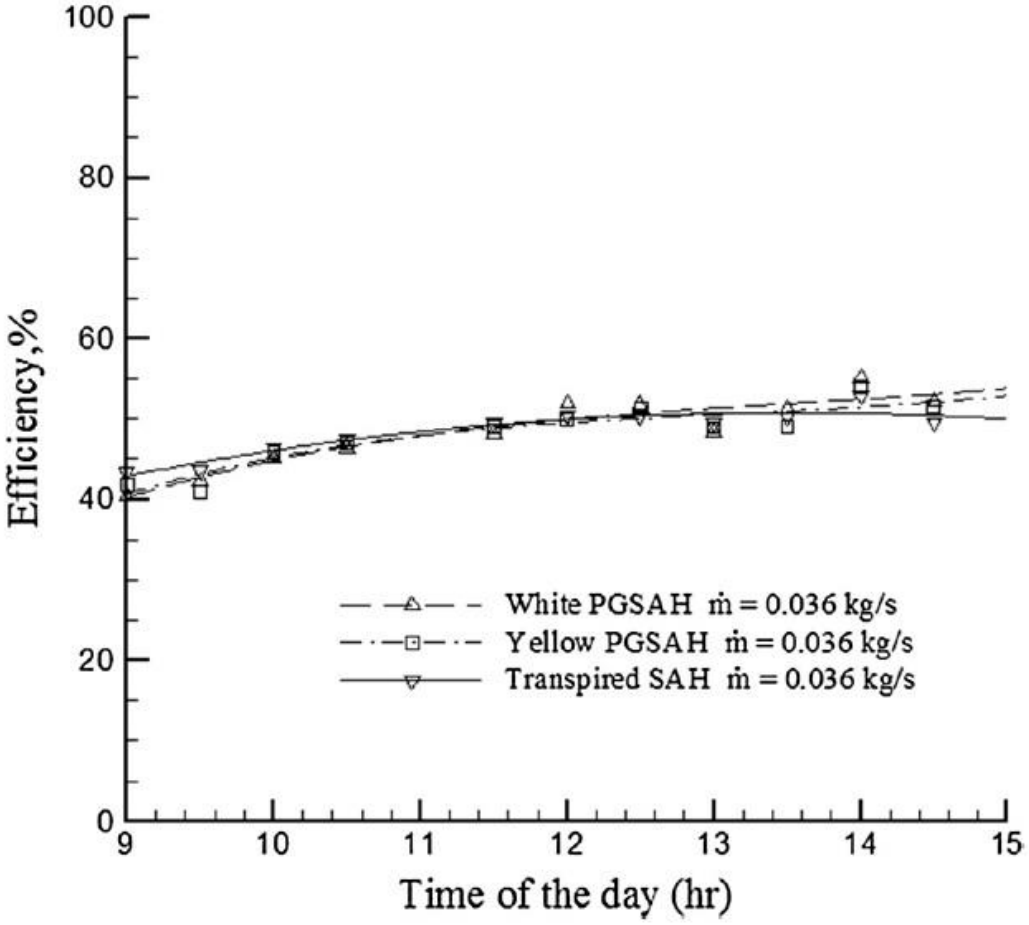

Figure 29: Efficiency of white PGSAH, yellow PGSAH and UTSAH versus time of the day for ṁ = 0.036 kg/s.

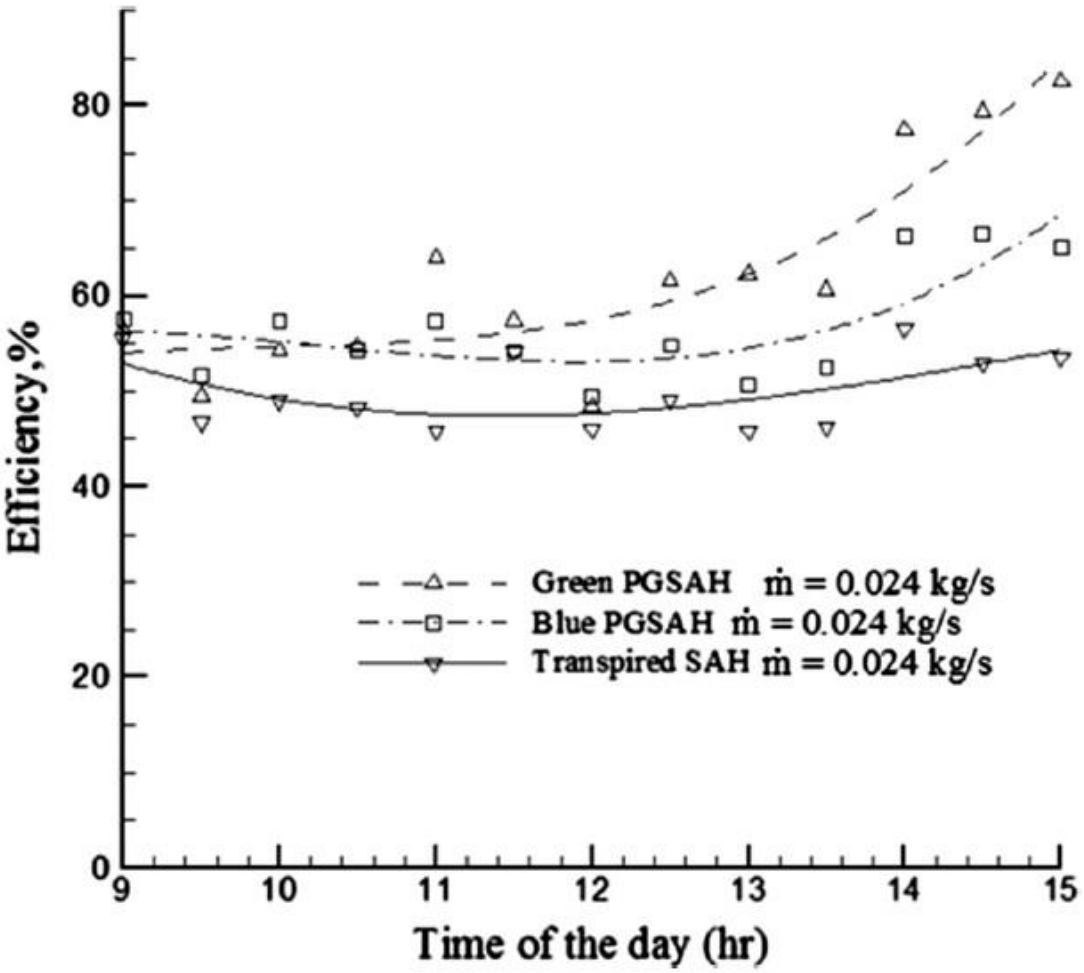

Figure 30: Efficiency of blue PGSAH, green PGSAH and UTSAH versus time of the day for ṁ = 0.024 kg/s.

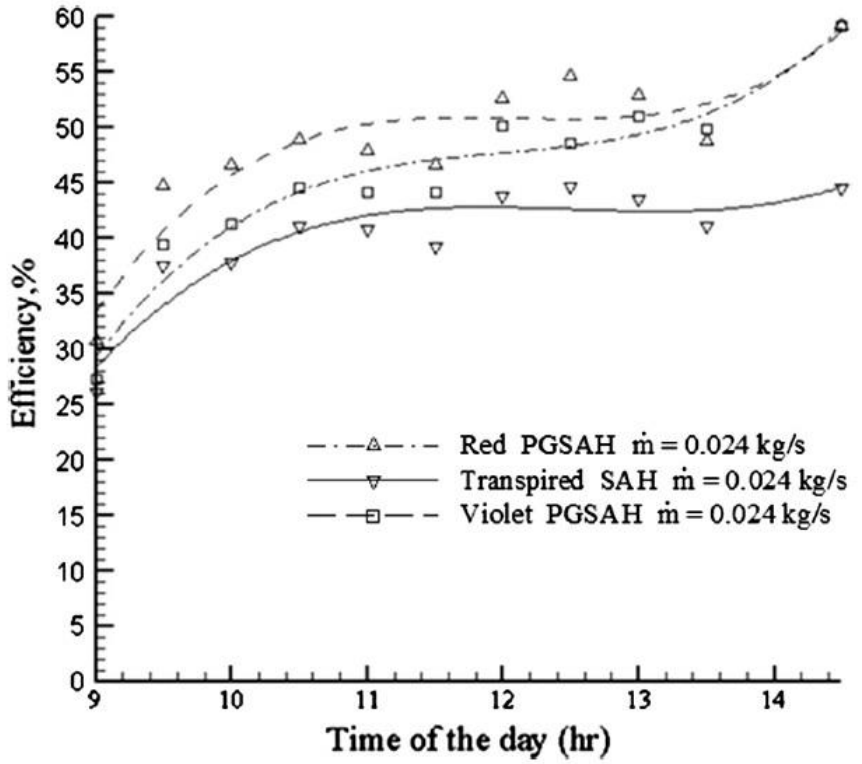

Figure 31: Efficiency of red PGSAH, violet PGSAH and UTSAH versus time of the day for ṁ = 0.024 kg/s.

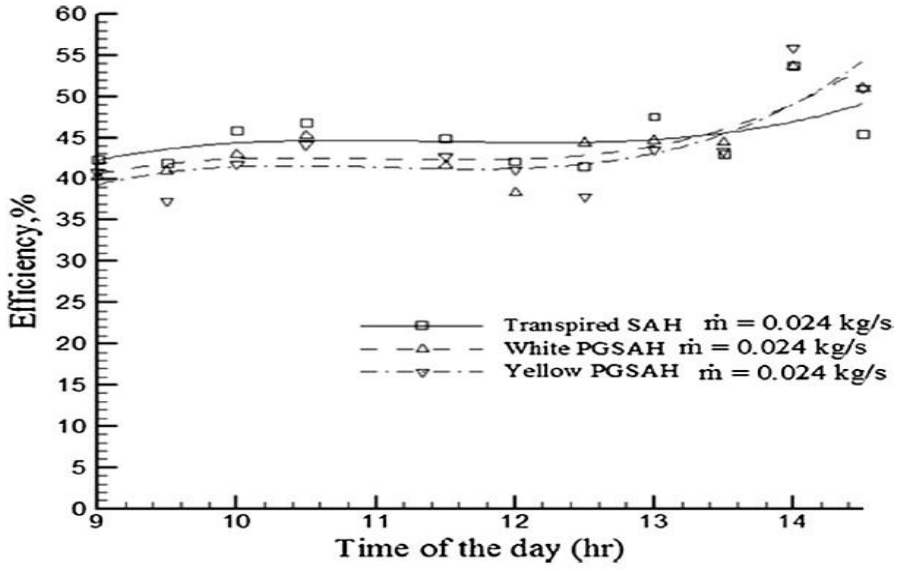

Figure 32: Efficiency of white PGSAH, yellow PGSAH and UTSAH versus time of the day for ṁ = 0.024 kg/s.

Figures 33 and 34, show the thermal efficiency increases by higher value of mass flow rate for different coloured PGSAHs.

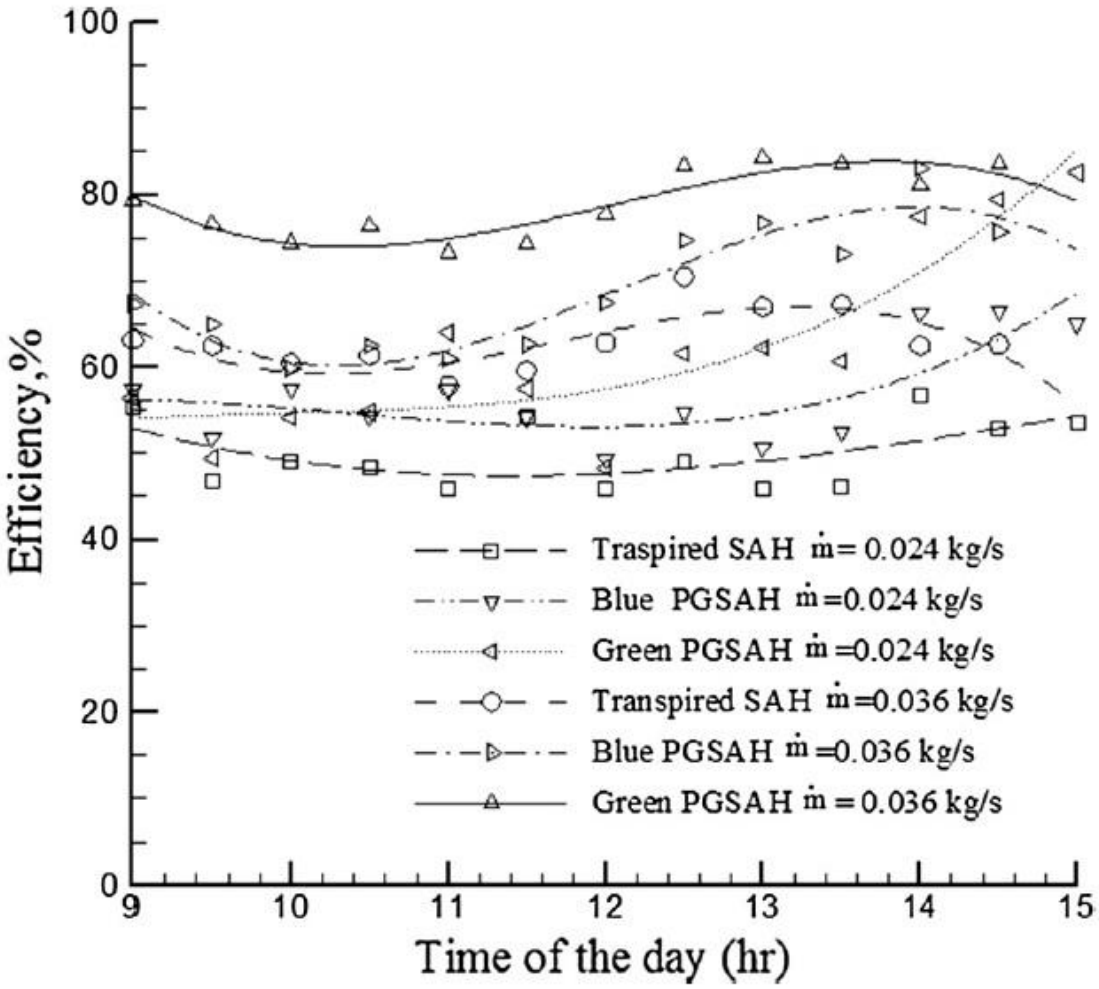

Figure 33: Efficiency of blue PGSAH, green PGSAH and UTSAH versus time of the day.

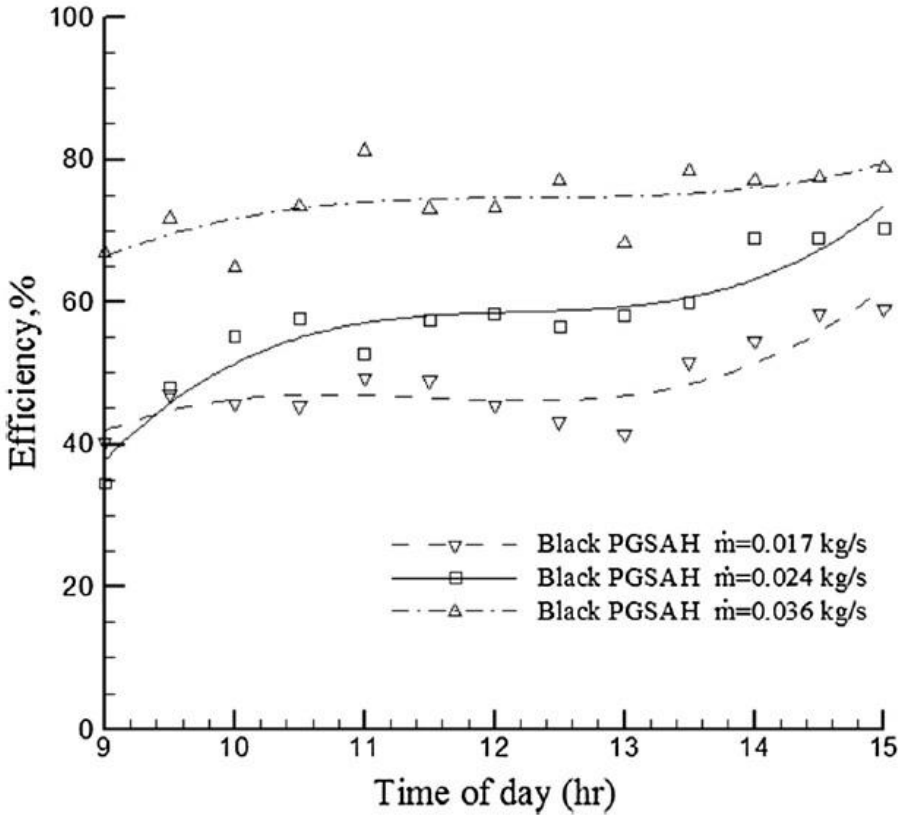

Figure 34: Efficiency of black PGSAH versus time of the day for various mass flow rates.

From Figure 35, the slopes of the efficiency curves increase while value of mass flow rate increases. Moreover, there is proportional relationship between thermal efficiency of black PGSAH' and ΔT/I ratio. Figure 36, demonstrates efficiency versus temperature rise parameter at various values of mass flow rate for blue PGSAH, green PGSAH and UTSAH. After black PGSAH, green PGSAH creates highest value of thermal efficiency among different coloured PGSAHs at maximum mass flow rate. Furthermore, thermal efficiency of PGSAH enhances as ΔT/I ratio increases.

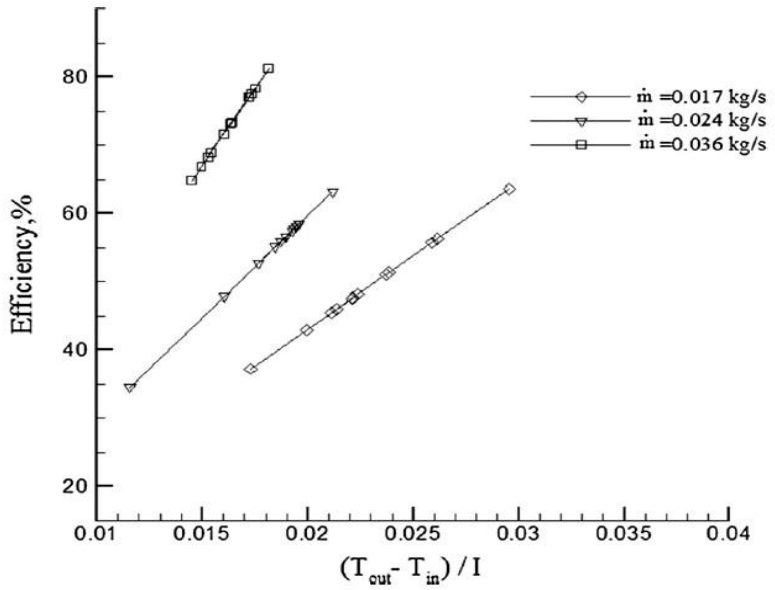

Figure 35: Efficiency versus temperature rise parameter at various mass flow rates for black PGSAH.

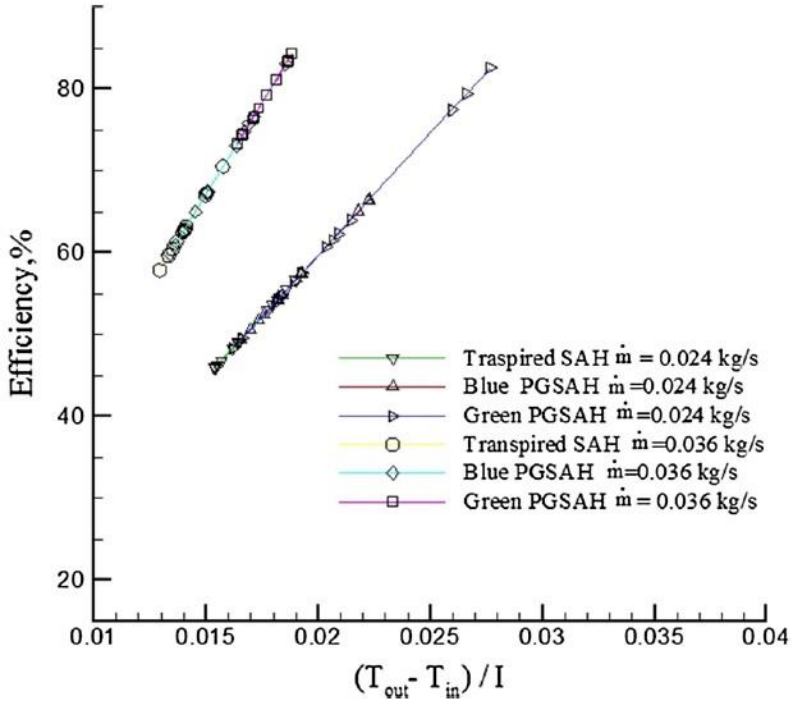

Figure 36: Efficiency versus temperature rise parameter at different mass flow rates for blue PGSAH, green PGSAH and UTSAH.

5.1.2. Uncertainty Analysis

In this section, uncertainties of ṁ and η are calculated. The mass flow rate (ṁ) is a function of three independent variables ṁ = f (T,V,A), which T as temperature, V as outlet air speed and A as a cross sectional area of exit. The mass flow rate is calculated as follows:

$$\dot{m} = \rho V A \tag{1}$$

where, ρ as density of air. The fractional uncertainty, $\frac{\omega_\eta}{\eta}$, for the mass flow rate is measured on the basis of book of Holman (1989):

$$\frac{\omega_{\dot{m}}}{\dot{m}} = \left[\left(\frac{\omega_{T_{air}}}{T_{air}}\right)^2 + \left(\frac{\omega_V}{V}\right)^2 + 4\left(\frac{\omega_r}{r}\right)^2\right]^{1/2} \tag{2}$$

which, T_{air} and r represent temperature of the film air and radius of pipe**.**

Moreover, SAH's thermal efficiency, η, is described as ratio of obtained energy to solar radiation incident on the cover of collector which is calculated as:

$$\eta = \frac{\dot{m} C_P (T_{out} - T_{in})}{I A_c} \tag{3}$$

where C_p, I and A_c represent specific heat of the air, solar intensity and area of the SAH. Furthermore, $\frac{\omega_\eta}{\eta}$ represents the fractional uncertainty of efficiency which has a direct relationship with I, ṁ and ΔT. The fractional uncertainty of efficiency is:

$$\frac{\omega_\eta}{\eta} = \left[\left(\frac{\omega_{\dot{m}}}{\dot{m}}\right)^2 + \left(\frac{\omega_{\Delta T}}{\Delta T}\right)^2 + \left(\frac{\omega_I}{I}\right)^2\right]^{1/2} \tag{4}$$

The fractional uncertainties of mass flow rate and thermal efficiency are calculated by utilizing the uncertainties related to the measurements of the parameters.

In addition, the fractional uncertainties of T_{air}, V, r, ΔT and I, are 0.0016, 0.0021, 0.005, 0.035 and 6.55×10^{-6} respectively. The calculations show that percent uncertainties in the mass flow rate and thermal efficiency for air mass flow rate of 0.036 kg/s are 1.05% and 3.65%, respectively.

5.2. Analysis of Thermal Performance of DPGSAHPB

Figure 37 illustrates solar intensity versus standard local time of the day among the certain days which experiments was accomplished. The mean value of solar intensity is calculated for each day. As can be seen from the Figure 37, the solar intensity enhances from the early morning to a maximum value at noon time. The maximum daily solar radiation intensity recorded was 990.48 W/m^2 at12:30h and the average solar intensity among that specific day was around 810.2 W/m^2.

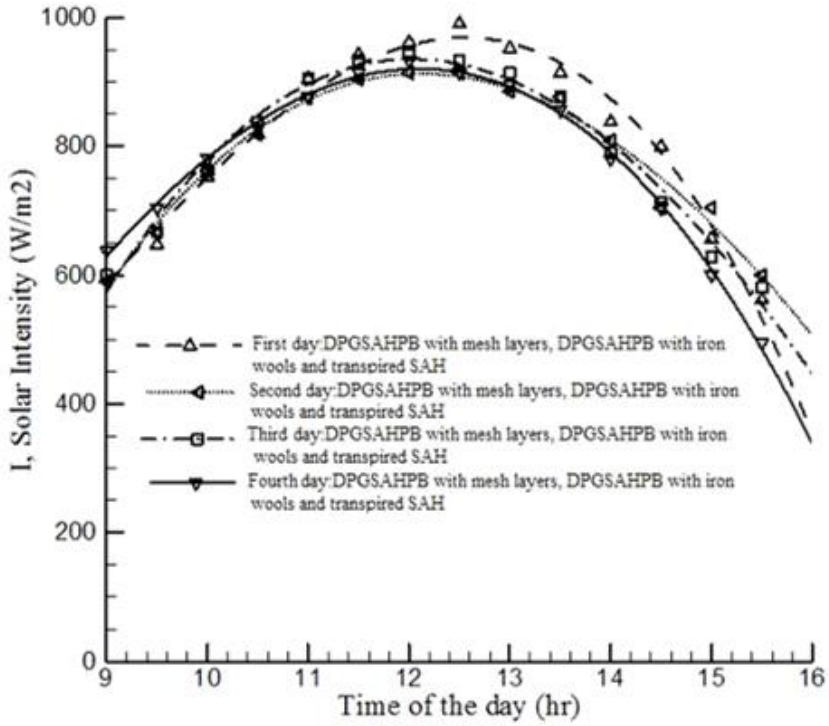

Figure 37: Solar intensity versus different standard local time of days for DPGSAHPB with mesh layers, DPGSAHPB with iron wools and UTSAH on four different days.

In Figures 38-41, ΔT versus time of day for DPGSAHPB with mesh layers and DPGSAHPB with iron wools and UTSAH for various air mass flow rates from (0.014 - 0.033) kg/s are illustrated.

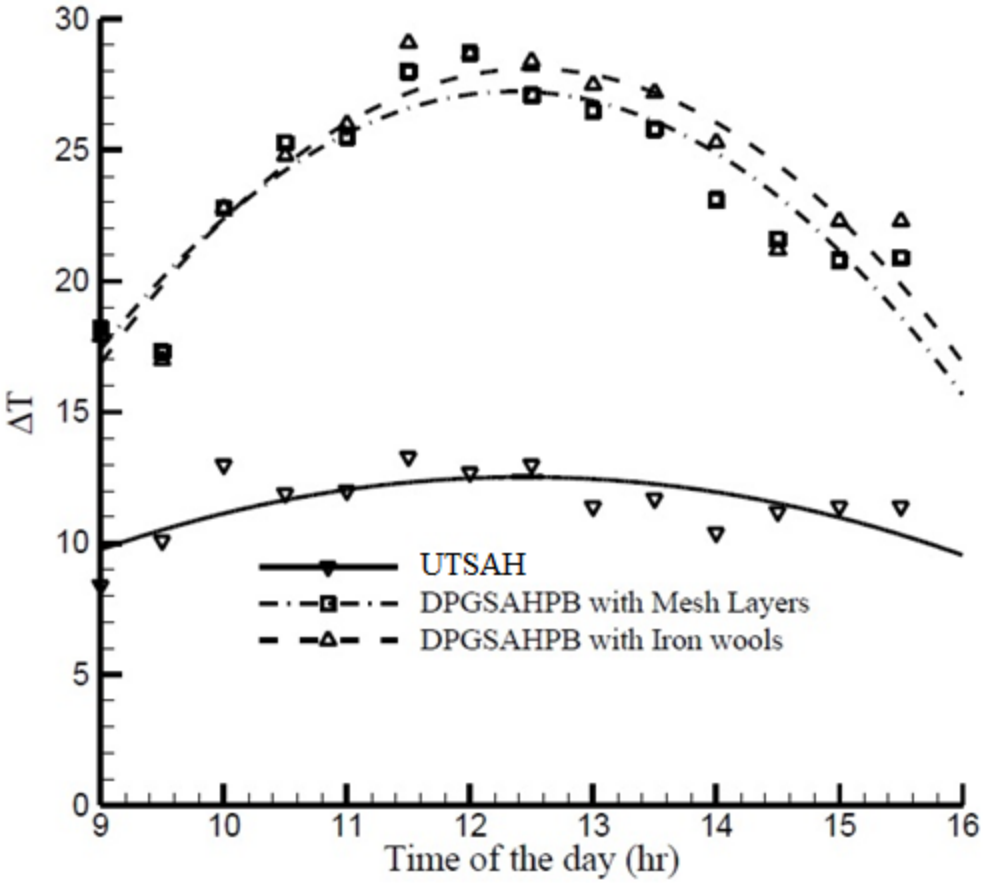

Figure 38: Variations of exit and inlet air temperature difference versus time of the day for DPGSAHPB with mesh layers, DPGSAHPB with iron wools and UTSAH for ṁ=0.014 kg/s.

The experimental results revealed that ΔT increases with decrease of mass flow rate. Furthermore, ΔT becomes maximum value for SAHs at noon time. Moreover, the highest of ΔT was obtained for DPGSAHPB with iron wools was 29.1℃ at 11:30 with a air flow rate of 0.014 kg/s.

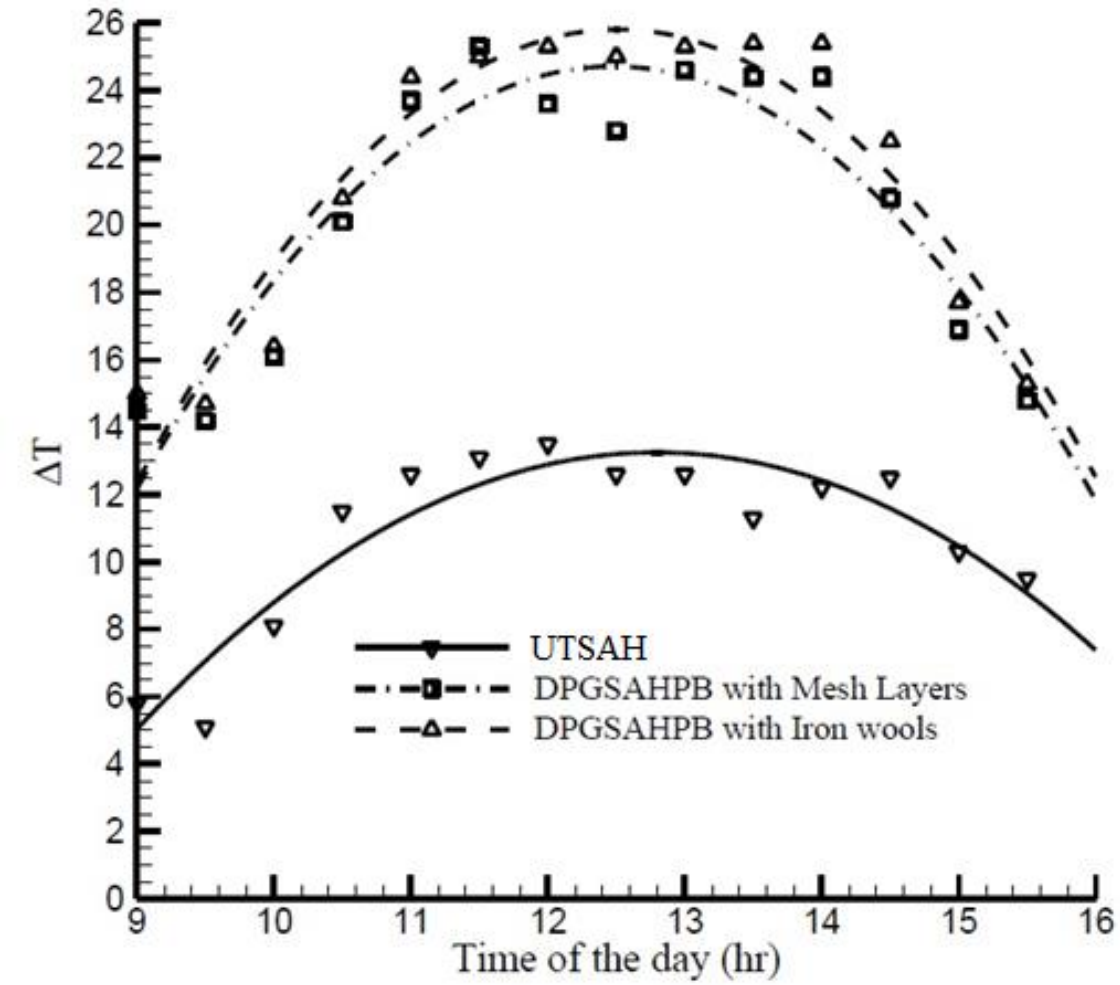

Figure 39: Variations of exit and inlet air temperature difference versus time of the day for DPGSAHPB with mesh layers, DPGSAHPB with iron wools and UTSAH for $\dot{m}$ =0.018 kg/s.

As can be seen from the figures, DPGSAHPB with iron wools produces higher value of ΔT compare with DPGSAHPB with mesh layers and also DPGSAHPB has higher ΔT than UTSAH.

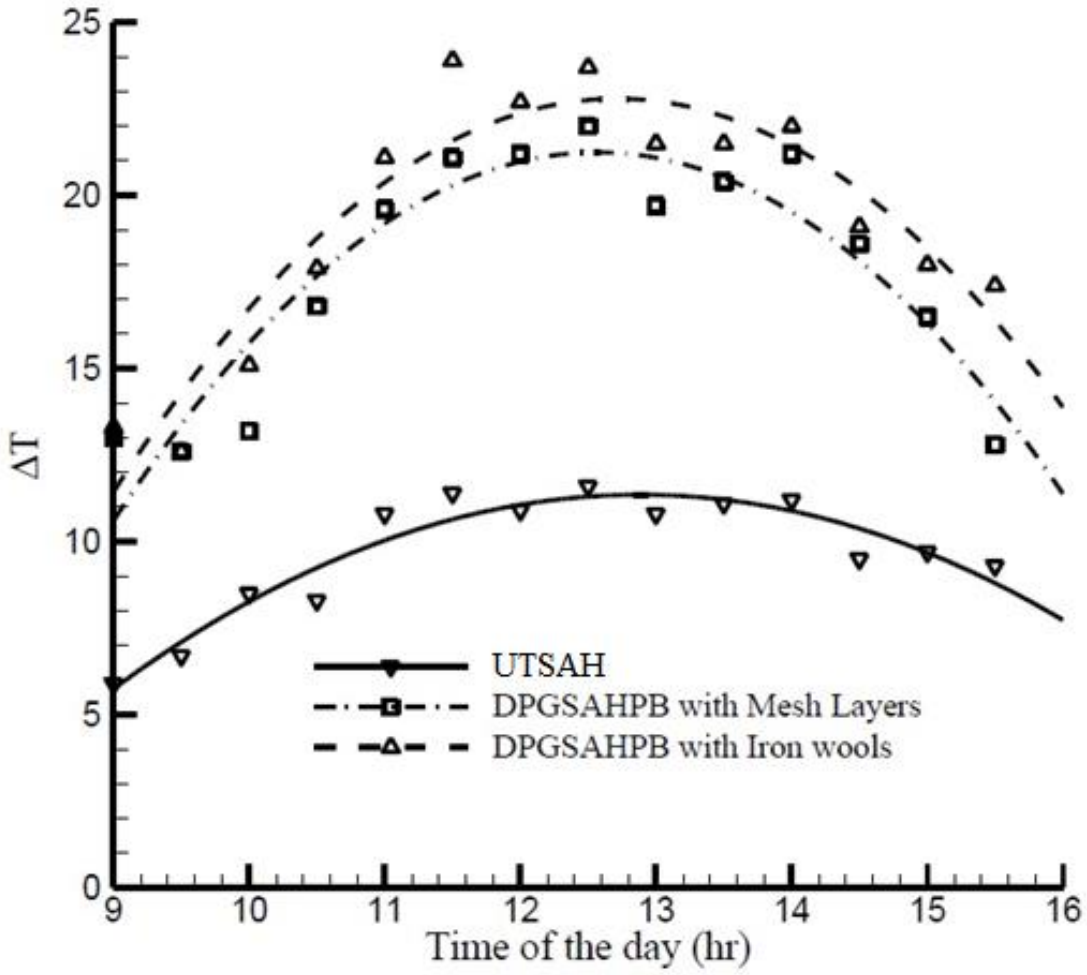

Figure 40: Variations of exit and inlet air temperature difference versus time of the day for DPGSAHPB with mesh layers, DPGSAHPB with iron wools and UTSAH for mass flow rate of 0.024 kg/s.

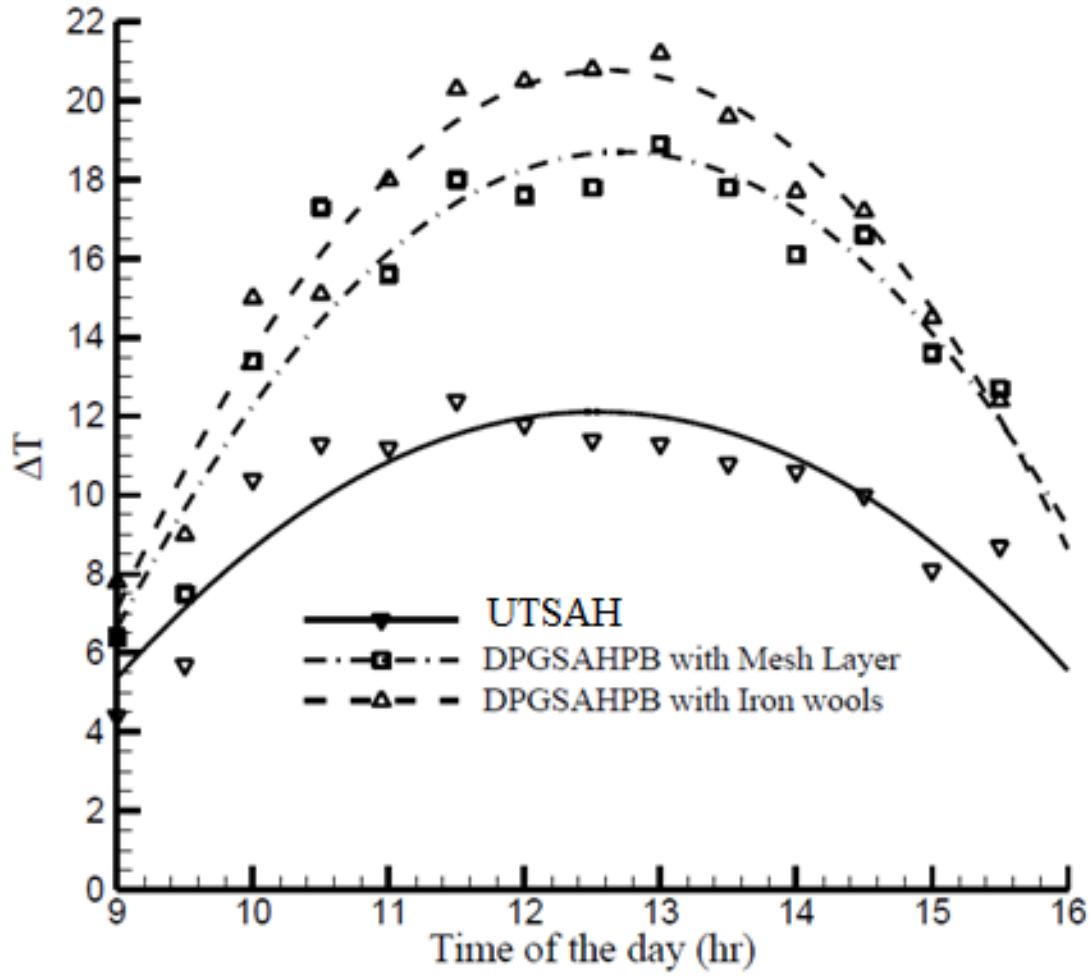

Figure 41: Variations of exit and inlet air temperature difference versus time of the day for DPGSAHPB with mesh layers, DPGSAHPB with iron wools and UTSAH for mass flow rate of 0.033 kg/s

Figuers 42-45 present the thermal efficiency versus the standard local time of the day at various mass flow rates for DPGSAHPB with mesh layers and DPGSAHPB with iron wools and UTSAH. It is demonstrated that thermal efficiency enhances by as air mass flow rate increases for same porosity of packing material (Figure 46). The diagrams illustrated that DPGSAHPB with iron wools is more efficient than DPGSAHPB with mesh layers and also thermal efficiency of DPGSAHPBs are higher than UTSAH.

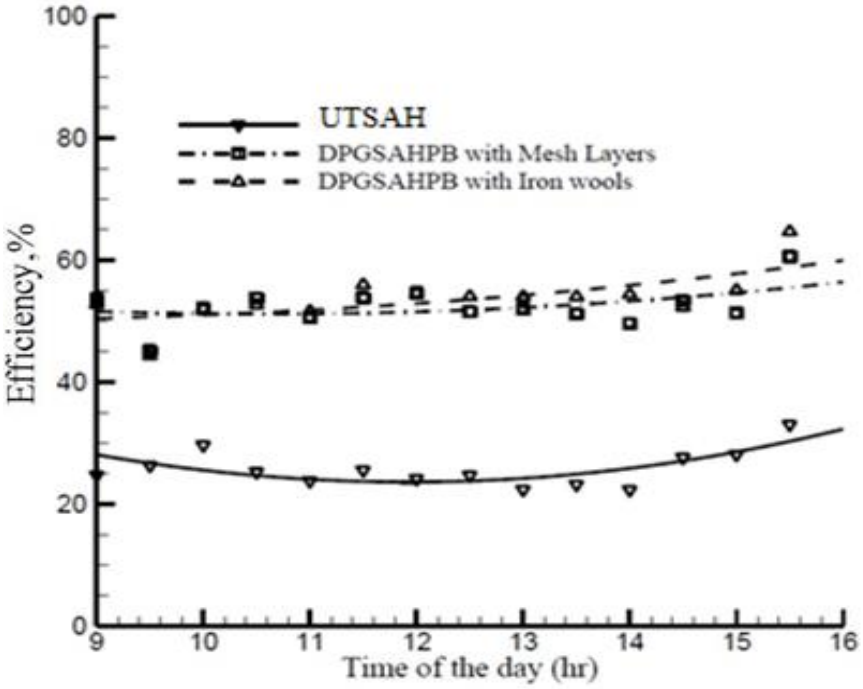

Figure 42: Efficiency of DPGSAHPB with mesh layers, DPGSAHPB with iron wools and UTSAH versus time of the day for mass flow rate of 0.014 kg/s.

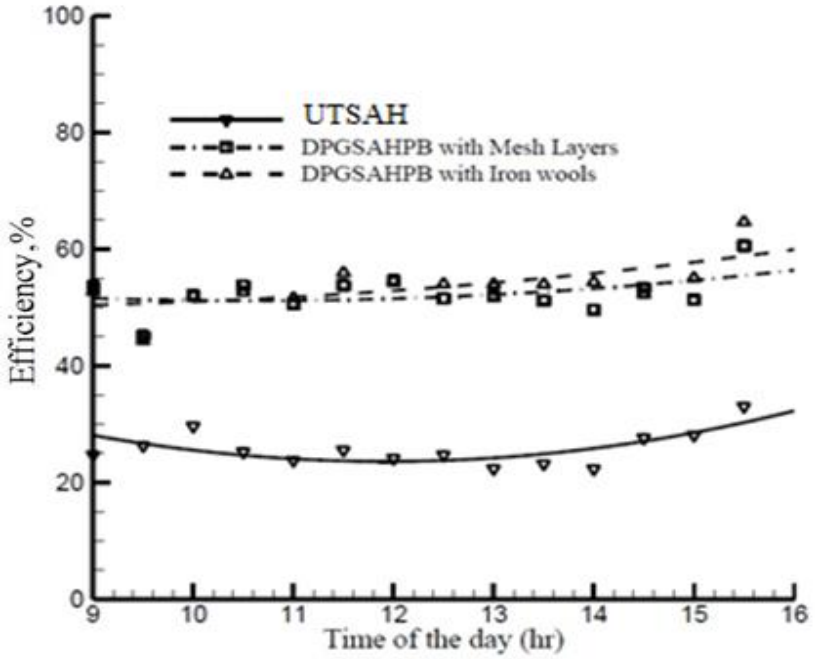

Figure 43: Efficiency of DPGSAHPB with mesh layers, DPGSAHPB with iron wools and UTSAH versus time of the day for mass flow rate of 0.018 kg/s.

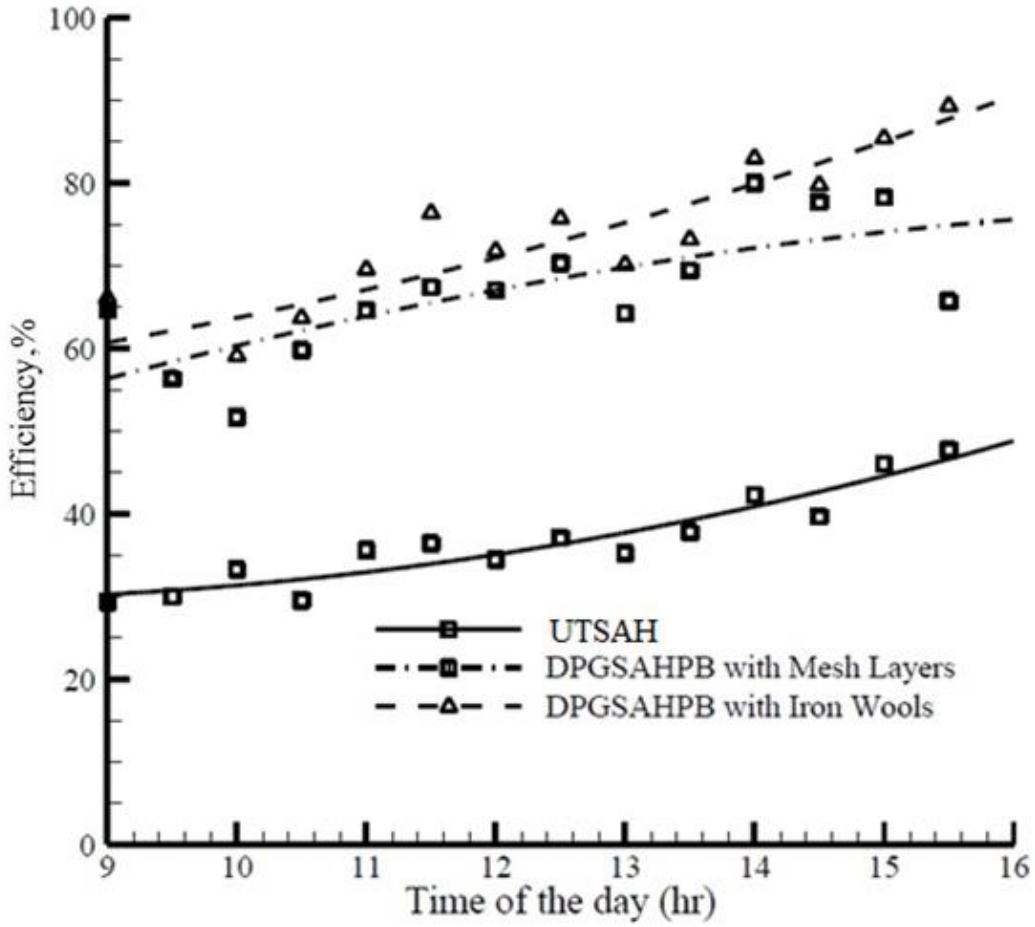

Figure 44: Efficiency of DPGSAHPB with mesh layers, DPGSAHPB with iron wools and UTSAH versus time of the day for mass flow rate of 0.024 kg/s.

The highest value of thermal efficiency for DPGSAHPB with iron wools was 91.3237% at maximum flow rate of 0.033 kg/s. It was also observed that there was a great difference between the efficiency of DPGSAHPBs and UTSAH but the thermal efficiency of DPGSAHPB with mesh layers and DPGSAHPB with iron wools are similar to each other. In addition, the average thermal efficiency obtained from the DPGSAHPB with mesh layers and DPGSAHPB with iron wools and transpired SAH were 75.1%, 81.9%, and 49.73% respectively for highest air mass flow rate of 0.033 kg/s.

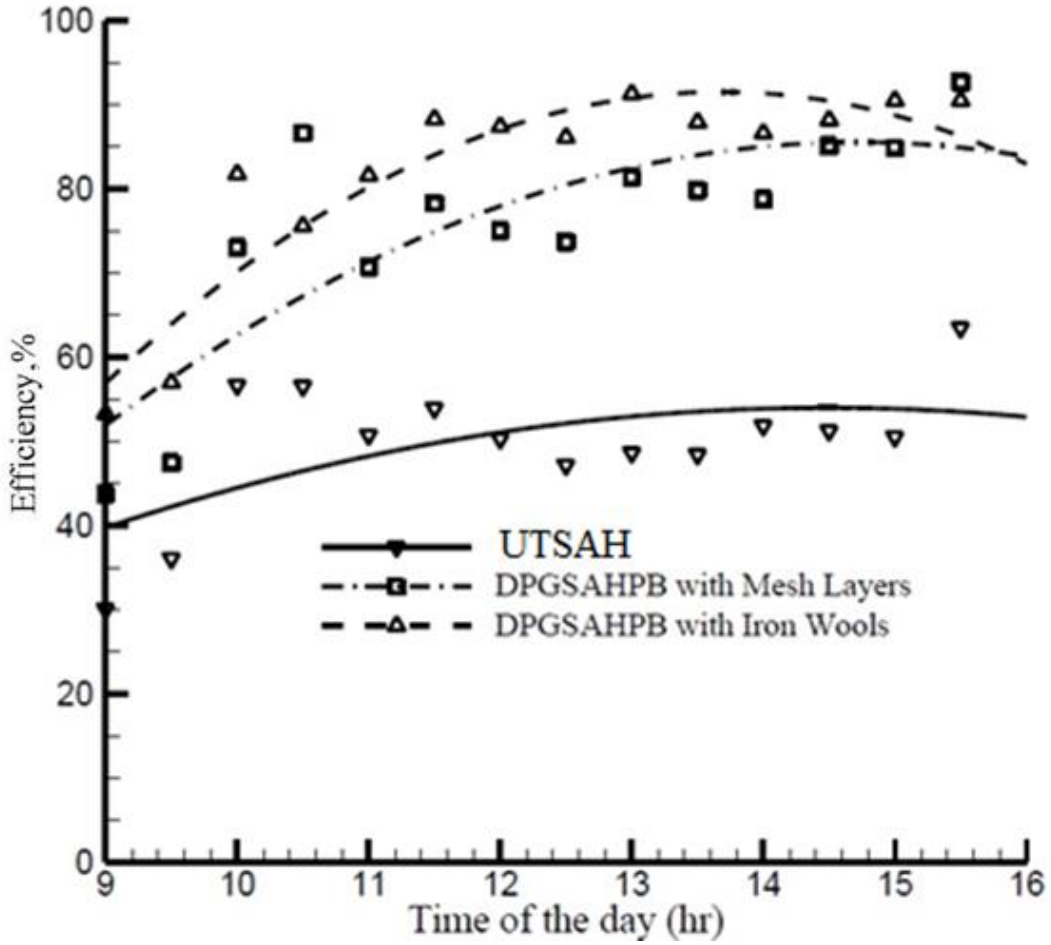

Figure 45: Efficiency of DPGSAHPB with mesh layers, DPGSAHPB with iron wools and UTSAH versus time of the day for mass flow rate of 0.033 kg/s.

The thermal efficiency of DPGSAHPB with iron wools and DPGSAHPB with mesh layers are each higher than transpired SAH for the same mass flow rate. The highest value of thermal efficiency is achieved by DPGSAHPB with iron wools which was 90% at the maximum mass flow rate of 0.033 kg/s.

The maximum values of thermal efficiencies for DPGSAHPB with iron wools and transpired SAH are calculated as 82% and 54% at $\dot{m}$=0.033 kg/s at noon time, respectively.

Figures 46 illustrates that average thermal efficiency increases with increase of mass flow rate for DPGSAHPBs and UTSAH.

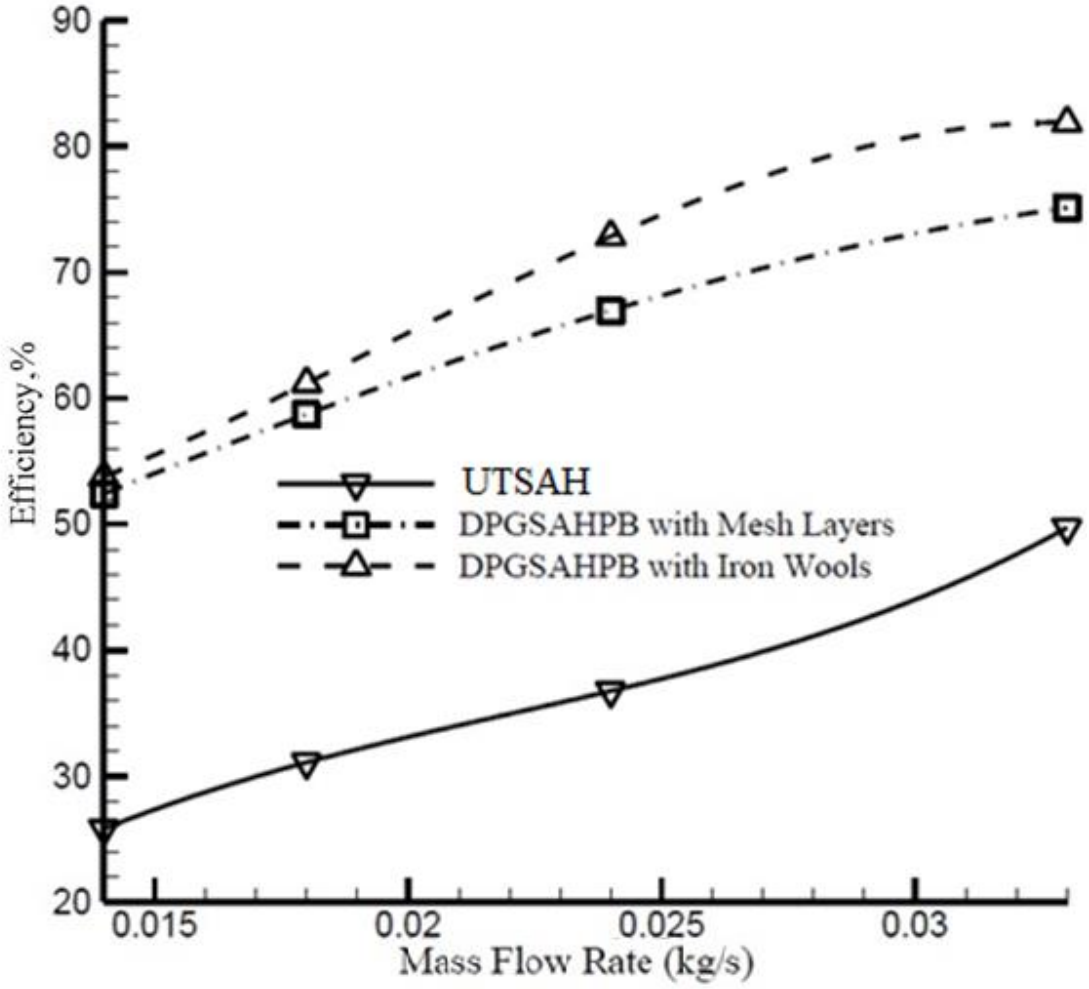

Figure 46: Average thermal efficiency versus different mass flow rates for DPGSAHPB with mesh layers and DPGSAHPB with iron wools and UTSAH

Figures 47 shows that thermal efficiency of DPGSAHPB with iron wools increases with increase of mass flow rates.

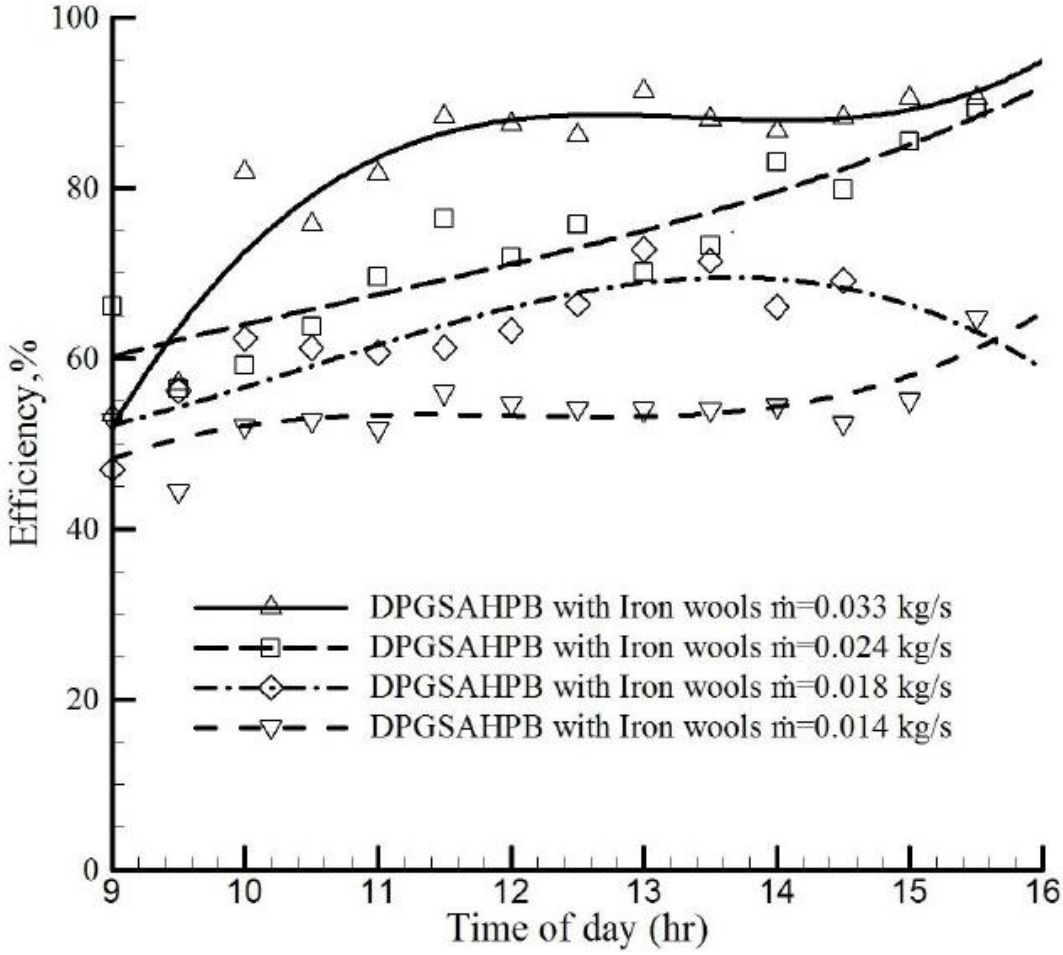

Figure 47: Efficiency of DPGSAHPB with iron wools versus time of the day for various mass flow rates

Figure 48, identifies that the slopes of the efficiency curves increase as mass flow rate enhances and also while ΔT/I ratio increases, the thermal efficiency of DPGSAHPB with iron wools enhances.

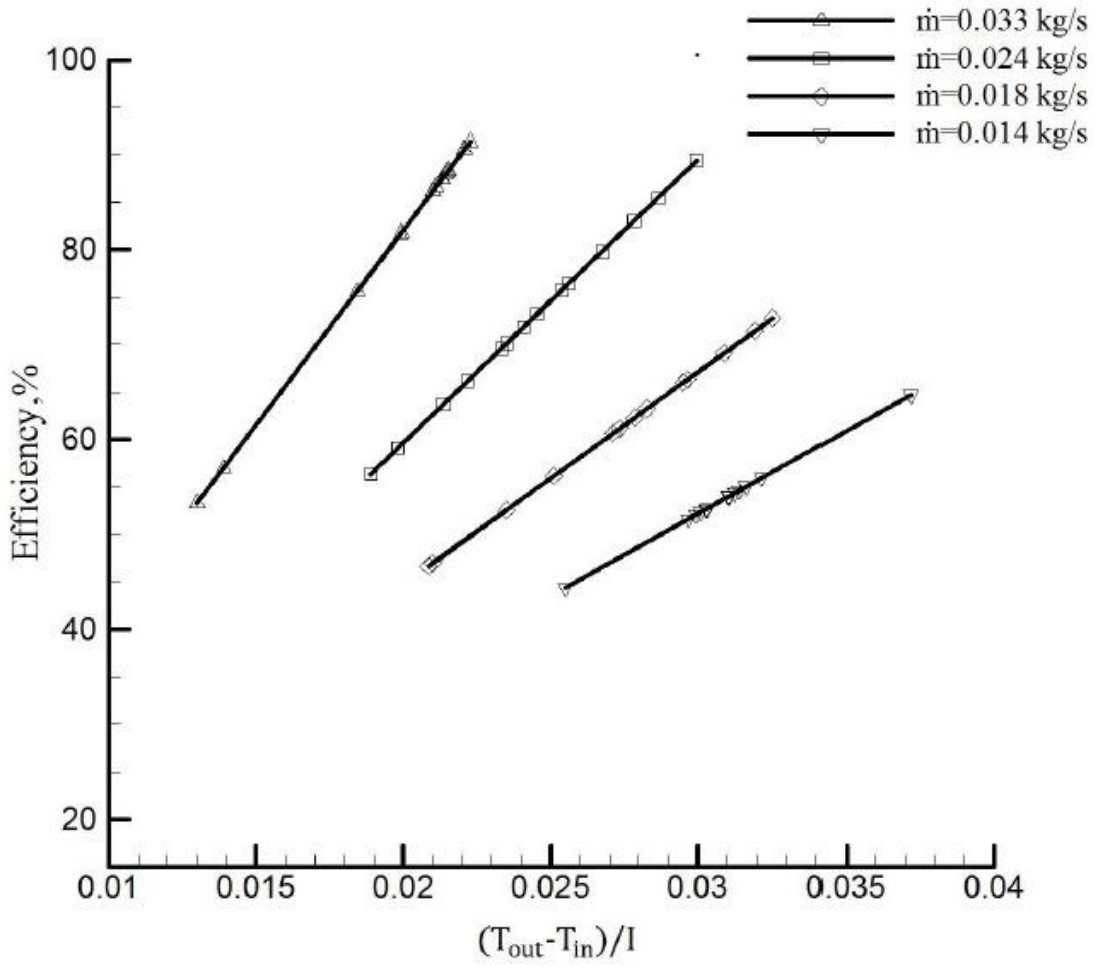

Figure 48: Efficiency versus temperature rise parameter at various mass flow rates for DPGSAHPB with iron wools

Figure 49 demonstrates efficiency versus temperature rise parameter at different mass flow rates for DPGSAHPB with mesh layers, DPGSAHPB with iron wools and transpired SAH. It is found that the efficiency of DPGSAHPB with mesh layers has the second highest value at maximum mass flow rate compared with other solar air heaters and increases at higher ΔT/I ratio.

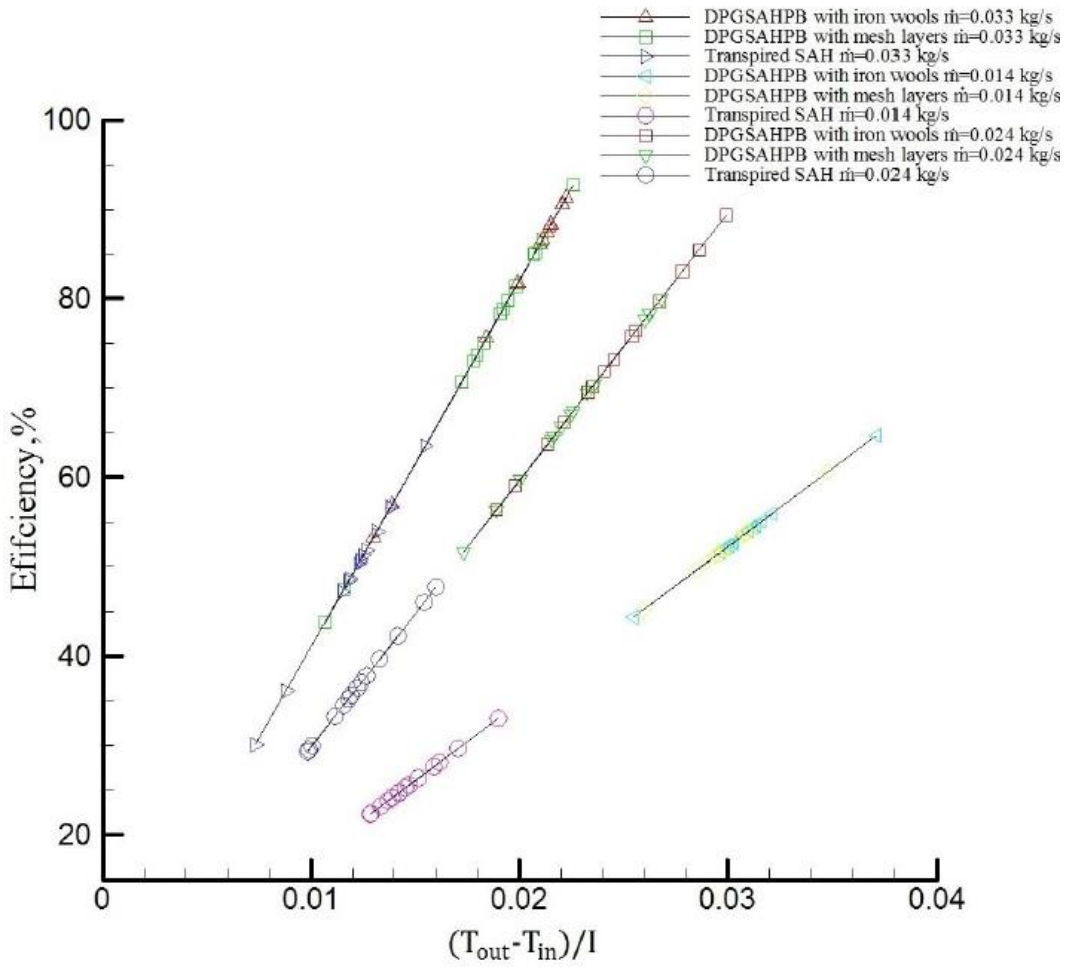

Figure 49: Efficiency versus temperature rise parameter at various mass flow rates for DPGSAHPB with mesh layers and DPGSAHPB with iron wools and UTSAH

5.2.2 Uncertainty Analysis

For second section of experiments, the fractional uncertainties of mass flow rate and efficiency are calculated by utilizing the uncertainties associated with the measurements of the parameters as same as first part of experiments. The fractional uncertainties of T_{air}, V, r, ΔT and I, are 0.0016, 0.0013, 0.005, 0.025 and 5.7×10^{-6}, respectively.

The calculations show that percent uncertainties in the mass flow rate and efficiency for maximum $\dot{m}$, 0.033 kg/s, are measured to be 1.02% and 2.7%, respectively.

Chapter 6

CONCLUSION AND FUTURE WORK

6.1 Conclusions of Present Study

This experimental survey presents a novel and efficient SAH called PGSAH. The SAH thermal performance has been improved significantly. PGSAH consists of perforated plexi glass, air blower, collector and no absorber plate. It is clear from the results of experiments that by employing perforated glazing, heat loss is reduced and thermal efficiency of SAH is enhanced. The ambient air is drawn into the collector via holes on plexi glass by utilizing a radial fan which eliminate heat losses from the plexi glass. There were two different series of experiments which were done in different days in Famagusta, a city of Cyprus. For each of the experiments, the present survey has different ambitions.

6.1.1 Conclusions of First Series of Experiments

In this section, experimental results regarding the performance of SPGSAHs having different inner collector colours and a black coloured UTSAH are demonstrated and analyzed. The fundamental conclusions are derived from current survey are as follows:

1. The SAH's efficiency enhances substantially by utilizing PGSAH

2. The thermal efficiencies of SPGSAHs (black, green, blue, red and violet) are each significantly better than that of UTSAH.

3. The thermal efficiencies of green and blue PGSAHs are close to the black PGSAH, which has maximum efficiency.

4. For SPGSAHs where light colours were used (yellow and white), thermal efficiencies were almost close to the efficiency of UTSAH for same mass flow rates.

5. With increase of mass flow rate, the thermal efficiency increases, but the temperature difference decreases.

6. The results illustrated that the thermal efficiency of dark coloured PGSAHs was better than the light coloured ones as expected.

The first series of experiments was concerned with the point of view that PGSAHs having different inner collector colours without any absorber plate compared the UTSAH illustrate preferable and acceptable thermal performances. As mentioned earlier, by using different coloured SPGSAHs the aesthetics of building facades and roofs can be improved.

6.1.2 Conclusions of Second Series of Experiments

In the second part of the experimental investigation, thermal performances of two different types of DPGSAHPB and UTSAH were analyzed under mass flow rates of 0.014, 0.018, 0.024, 0.033 kg/s. Eventually, the results achieved can be summarized as follows:

1-The perforated glazed solar air heaters are more efficient than conventional SAH's due to less heat loss from the perforated glazing.

2- DPGSAHPB creates higher outlet temperature compared with conventional SAH and also they are more efficient than PGSAHs.

3- By utilizing iron wools and wire mesh layers as packed bed, the efficiencies were improved. The thermal efficiency of DPGSAHPB with iron wools is higher than DPGSAHPB with wire mesh layers.

4-Thermal efficiency of both type of DPGSAHPBs are greater than UTSAH under the same conditions.

5-The highest thermal efficiency is achieved by DPGSAHPB with iron wools at maximum air mass flow rate and also the lowest thermal efficiency was achieved by the UTSAH at minimum air mass flow rate.

6.2 Future Work

For future studies, various modifications can be made such as the sizes of collectors, use of different pitch, different hole diameters, different plexiglass thichness to study the impact on the efficency. It is also a proper idea to use a parabolic perforate glazed solar air heater to increase the thermal performance.

REFERENCES

Adnane, L., Noureddine, M., & Adel, B. (2012). Experimental investigation of various designs of solar flat plate collectors: Application for the drying of green chili. *Journal of Renewable and Sustainable Energy*. 4(4). doi: 10.1063/1.4742337

Ahmad, A., Saini, J. S., & Varma (1996). Thermohydraulic performance of packed-bed solar air heaters. *Energy Conversion and Management.* 37, 205-214.

Akpinar, E. K., & Koçyiğit, F. (2010). Experimental investigation of thermal performance of solar air heater having different obstacles on absorber plates. *International Communications in Heat and Mass Transfer*. 37, 416–421.

Aldabbagh, L.B.Y., Egelioglu, F., & Ilkan, M. (2010). Single and double pass solar air heaters with wire mesh as packing bed. *Energy*. 35, 3783-3787.

Alejandro, L. H., & José, E. Q. (2013). Analytical models of thermal performance of solar air heaters of double-parallel flow and double-pass counter flow. *Renewable Energy*. 55, 380–391.

Alta, D., Bilgili, E., Ertekin, C., & Yaldiz, O. (2010). Experimental investigation of three different solar air heaters: Energy and exergy analyses. *Applied Energy*. 87, 2953–2973.

Anandh, A., & Baskar, R. (2015). Experimental investigation of double pass solar air heater using different porous media. *International Journal for Scientific Research & Development*.3.

Anderson, T.N., Duke, M., & Carson, J.K. (2010). The effect of colour on the thermal performance of building integrated solar collectors. *Solar Energy Materials & Solar Cells*. 94, 350–354.

Arulanandam, S.J., Hollands, K.G.T., & Brundrett, E. (1997). A CFD heat transfer analysis of the transpired solar collector under no-wind conditions. *Solar Energy*. 67, 93–100.

Bahrehmand, D., & Ameri, M. (2015). Energy and exergy analysis of different solar air collector systems with natural convection. *Renewable Energy*. 74, 357-368.

Bansal, N.K., Boettcher, A., & Uhlemann, R. (1983). Performance of plastic solar air. heating collectors with a porous absorber. *International Journal of Energy Research*. 7, 375–384.

Bayrak, F., Oztop, Hakan, F., & Hepbasli, A. (2013). Energy and exergy analyses of porous baffles inserted solar air heaters for building applications. *Energy and Build*. 57, 338–345.

Brij, B., & Ranjit, S. (2012). Thermal and thermohydraulic performance of roughened solar air heater having protruded absorber plate. *Solar Energy*. 86, 3388–3396.

Chabane, F., Moummi, N., & Benramache, S. (2013). Experimental analysis on thermal performance of a solar air collector with longitudinal fins in a region of Biskra, Algeria. *Journal of Power Technologies*. 93 (1), 52–58.

Chabane, F., Moummi, N., & Benramache, S. (2014). Experimental study of heat transfer and thermal performance with longitudinal fins of solar air heater. *Journal of Advanced Research*. 5,183-192.

Chamoli, S., Chauhan, R., Thakur, N.S., & Saini, J.S. (2012). A review of the performance of double pass solar air heater. *Renewable and Sustainable Energy Reviews.* 16, 481– 492.

Chii-Dong, Ho, Chun-Sheng, Lin, Yu-Chuan, Chuang, & Chun-Chieh, Chao (2013). Performance improvement of wire mesh packed double-pass solar air heaters with external recycle. *Renewable Energy*. 57, 479-489.

Chii-Dong, Ho, Hsuan, Ch., Chun-Sheng, Lin, Chun-Chieh, Chao, & Yi-En, Ti. (2015). Analytical and experimental studies of wire mesh packed double-pass solar air heaters under recycling operation. *Energy Procedia*. 75, 403 – 409.

Christensen, C., Hancock, E., Barker, G., & Kutscher, C. (1990). Cost and performance predictions for advanced active solar concepts. *USA: American Solar Energy Society*. 275-280.

Ekenchukwu, O. V., & Norton B. (1999). Review of solar-energy drying systems III: low temperature air-heating solar collectors for crop drying applications. *Energy Conversion & Management*. 40, 657-667.

El-khawajah, M.F., Egelioglu, F., & Aldabbagh, L.B.Y. (2011). The effect of using transverse fins on a double pass flow solar air heater using wire mesh as an absorber. *Journal of Solar Energy*. 85, 1479–1487.

El-Sebaii, A.A., Aboul-Enein, S., Ramadan, M.R.I., & El-Bialy, E. (2007). Year round performance of double pass solar air heater with packed bed. *Energy Conversion and Management*. 48, 990–1003.

El-Sebaii, A.A., Aboul-Enein, S., Ramadan, M.R.I., Shalaby, S.M., & Moharram, B.M. (2011). Thermal performance investigation of double pass-finned plate solar air heater. *Applied Energy*. 88, 1727–1739.

Energy Efficiency Trends and Policies in the Household and Tertiary Sectors, An Analysis Based on the ODYSSEE and MURE Databases. (2015, June 15). Retrieved from http://www.odyssee-mure.eu/publications/br/energy-efficiency-in-buildings.html.

Esen, H. (2008). Experimental energy and exergy analysis of a double-flow solar air heater having different obstacles on absorber plates. *Building and Environment*. 43, 1046–1054.

Fudholi, A., Sopian, K. Z., Ruslan, M. H., & Othman, M. Y. (2013). Performance and cost benefits analysis of double-pass solar collector with and without fins. *Energy Conversion and Management*. 76, 8–19.

Gao, L., & Fang, X. (2011). Numerical Simulation of the Thermal Performance of Solarwall. Measuring Technology and Mechatronics Automation (ICMTMA), Third International Conference on 2011, 721-724.

Gholampour, M. & Ameri, M. (2014). Design Considerations of Unglazed Transpired Collectors: Energetic and Exergetic Studies. *Journal of Solar Energy Engineering*. 136(3).

Gill, RS., Singh, S., & Singh, P.P. (2012). Low cost solar air heater. *Energy Conversion and Management*. 57, 131‑42.

Giovanni, T. (2011). Performance of solar air heater ducts with different types of ribs on the absorber plate. *Energy*. 36, 6651-6660.

Hans, V.S., Saini, R.P., & Saini, J.S. (2010). Heat transfer and friction factor correlations for a solar air heater duct roughened artificially with multiple v-ribs. *Solar Energy*. 84, 898–911.

Hikmet, E. (2008). Experimental energy and exergy analysis of a double-flow solar air heater having different obstacles on absorber plates. *Building and Environment*. 43, 1046–1054.

Ho, C.D., Yeh, H.M., & Wan, R.C. (2005). Heat-transfer enhancement in double-pass flat-plate solar air heaters with recycle. *Energy*. 30, 2796–2817.

Hollick, J.C. (1994). Unglazed solar wall air heaters. *Renewable Energy*. 5, 415–421.

Hollick, J.C. (1998). Solar cogeneration panels. *Renewable Energy.* 15, 195–200.

Holman, J. (1989). Experimental Methods for Engineers, seventh ed. McGraw-Hill, New York.

IEA. Heat Pump Programme (2009). Heat pumps can cut global CO_2 emissions by nearly 8%. Heat Pump Centre, Sweden. (2015, july 13). Retrieved from http://heatpumpingtechnologies.org/

IEA. Energy and the challenge of sustainability. (2015, August 14). Retrieved from http://www.iea.org/publications/freepublications

Jesko, V. (2008). Classification of solar collectors. *Engineering For Rural Development*. 29, 30-35.

Jing-Li, F., Hao, Y., & Yi-Ming, W. (2015). Residential energy-related carbon emissions in urban and rural Chinaduring 1996–2012: From the perspective of five end-use activities. *Energy and Buildings*. 96, 201–209.

Kalogirou, S. (1997). Solar water heating in Cyprus: current status of technology and problems. *Renewable Energy*. 10, 107-112.

Karmare, S.V., & Tikekar, A.N. (2009). Experimental investigation of optimum thermohydraulic performance of solar air heaters with metal rib grits roughness. *Solar Energy*. 83, 6–13.

Kapardar, A. Kumar, & Sharma, Dr. R. P. (2012). Experimental investigation of solar air heater using porous medium. *International journal of mechanical engineering and technology*. 3, 387-396.

Krishnananth, S.S., & Murugavel, K. K. (2013). Experimental study on double pass solar air heater with thermal energy storage. *Engineering Sciences*. 25, 135–140.

Kumar, A., Saini, R.P., & Saini, J.S. (2014). A review of thermohydraulic performance of artificially roughened solar air heaters. *Renewable and Sustainable Energy Reviews*. 37, 100– 122.

Kurtbas, I., & Turgut, E. (2006). Experimental investigation of solar air heater with free and fixed fins: efficiency and exergy loss. *International Journal of Science & Technology*. 1, 75-82.

Kutscher, CF, Christensen, C, & Barker, G (1991). Unglazed transpired solar collectors - an analytical model and test-results. *Solar World Congress*, vol 1, Pts 1-2 ; vol 2, Pts 1-2 ; vol 3, Pts 1-2 ; 1245-1250.

Kutscher, C.F. (1996). Transpired solar collector systems: a major advance in solar heating. *Proceedings of the 19th World Energy Engineering Congress*, Atlanta, GA.

Lalji, M.K., Sarvia, R.M., & Bhagoria, J.L. (2011). Experimental investigations on packed bed solar air heater. *Current World Environment*. 6, 151-157.

Lertsatitthanakorn, C., Khasee, N., Atthajariyakul, S., Soponronnarit, S., Therdyothi, A., & Suzuki, R.O. (2008). Performance analysis of a double-pass thermoelectric solar air collector. *Solar Energy Materials and Solar Cells*. 92, 1105–1109.

McAdams, W.H. (1954). Heat transmission. New York: McGraw-Hill.

Mahmood, A.J., Aldabbagh, L.B.Y., & Egelioglu, F. (2015). Investigation of single and double pass solar air heater with transverse fins and a package wire mesh layer. *Energy Conversion and Management*. 89, 599‑607.

Martin, S.R.L., & Fjeld, G.J. (1975). Experimental performance of three solar collectors. *Energy*. 7, 345–349.

Michael, H., Xavier, L., José, M. L., & Xiral, L. (2013). Energy Demand for Heating: Short Run and Long Run. *economics for energy*.

Mittal, M.K., & Varshney, L. (2006). Optimal thermo hydraulic performance of a wire mesh packed solar air heater. *Solar Energy*. 80, 1112–1120.

Mohamad, A.A. (1977). High efficiency solar air heater. *Solar Energy*. 60, 71–76.

Motahar, S., & Alemrajabi, A.A. (2010). An analysis of unglazed transpired solar collectors based on exergetic performance criteria. *International Journal of Thermodynamics*.13, 153-160.

Nowzari, R., Aldabbagh, L.B.Y., & Egelioglu, F. (2014). Single and double pass solar air heaters with partially perforated cover and packed mesh. *Energy.* 73, 694-702.

NREL, a DOE National Laboratory, Transpired collectors (Solar preheaters for outdoor ventilation air, Washington:1998. (2015, july 17). Retrieved from http://www.nrel.gov/docs/fy06osti/29913.pdf.

NREL, a DOE National Laboratory, Solar Buildings Transpired Air Collectors Ventilation Preheating , Washington:2006. Retrived 5 july 2015 from: http://www.nrel.gov/docs/fy06osti/29913.pdf.

Omojaro, A.P., & Aldabbagh, L.B.Y. (2010). Experimental performance of single and double pass solar air heater with fins and steel wire mesh as absorber. *Applied Energy*. 87, 3759–3765.

Ozgen, F., Esen, M., & Esen, H. (2009). Experimental investigation of thermal performance of a double-flow solar air heater having aluminium cans. *Renewable Energy*. 34, 2391–2398.

Qenawy, A.M., & Mohamad, A.A. (2007). Analysis of high efficiency solar air heater for cold climates. Calgary, Canada: 2nd Canadian Solar Buildings Conference,10–14.

Paisarn N. (2005)a. On the performance and entropy generation of the double-pass solar air heater with longitudinal fin. *Renewable Energy*. 30, 1345–1357.

Paisarn, N. (2005)b. Effect of porous media on the performance of the double-pass flat plate solar air heater. *International Communication in Heat and Mass Transfer.* 32, 140–150.

Pavel, C., Milan, O., Tomas, M., & Lubomir, K. (2012). Solar air collector with integrated latent heat thermal storage. *EPJ Web of Conferences* 25.

Pottler, K., Sippel, C.M., Beck, A., & Fricke, J. (1999). Optimized finned absorber geometries for solar air heating collectors. *Solar Energy*. 67, 35–52.

Prasad, S.B., Saini, J.S., & Singh, K.M. (2009). Investigation of heat transfer and friction characteristics of packed bed solar air heater using wire mesh as packing material. *Solar Energy*. 83, 773–783.

Ramadan, M.R.I., ELSebaii, A.A., AboulEnein, S., & ElBialy, E. (2007). Thermal performance of a packed bed double-pass solar air heater. *Energy.* 32, 1524–1535.

Ramani, B.M., Akhilesh, G., & Ravi, K. (2010). Performance of a double pass solar air collector. *Solar Energy*. 84, 1929–1937.

Sanjay, Y., Maneesh, K., & Varun, S. (2014). Exergetic performance evaluation of solar air heater having arc shape oriented protrusions as roughness element. *Solar Energy*. 105, 181–189.

Singh, A. P., & Varun, S. (2014). Effect of artificial roughness on heat transfer and friction characteristics having multiple arc shaped roughness element on the absorber plate. *Solar Energy*. 105, 479–493.

Singh, S., & Dhiman, P. (2014). Thermal and thermohydraulic performance evaluation of a novel type double pass packed bed solar air heater under external recycle using an analytical and RSM (response surface methodology) combined approach. *Energy*. 72, 344-359

Smil, V. (1991). General Energetics: Energy in the Biosphere and Civilization. Wiley. p. 369. ISBN 0-471-62905-7.

SolarWall (2008). How solarwall technology works to provide fresh air and free heat, Conserval Engineering Inc. (2015, Febrerary 13). Retrieved from http://solarwall.com/en/products/solarwall-air-heating/how-it-works.php.

Sopian, K., Supranto, W.R.W., Daud, M.Y., & Othman, B.Y. (1999). Thermal performance of the double pass solar collector with and without porous media. *Renewable Energy*. 18, 557–564.

Sopian, K., Alghoul, M.A., Ebrahim, M., Sulaiman, M.Y., & Musa, E.A. (2009). Evaluation of thermal efficiency of double pass solar collector with porous nonporous media. *Renewable Energy*. 34, 640–645.

Thakur, N.S., Saini, J.S., & Solanki, S.C. (2003). Heat transfer and friction factor correlations for packed bed solar air heater for a lower porosity system. *Solar Energy*. 74, 319–329.

The annual energy outlook 2015 (AEO2015) with projections to 2040, April 2015.

The Heat Pump Centre (HPC), 2016. (2016, March 10). Retrieved from http://www.heatpumpcentre.org/en/Sidor/default.aspx.

Tiwari, G.N. (2002). Solar energy fundamentals, design, modelling and applications. Narosa Publishing House, New Delhi.

Tripanagnostopoulos, Y., Souliotis, M., & Nousia, T.H. (2000). Solar collectors with coloured absorbers. *Solar Energy*. 68, 343–356.

Ürge-Vorsatz, D., Cabeza, L.F., Serrano, S., Barreneche, & C., Petrichenko, K. (2015). Heating and cooling energy trends and drivers in buildings. *Renewable and Sustainable Energy Reviews*. 41, 85–98.

UNFCCC secretariat, 2015. Paris Agreement, FCCC/CP/2015/L.9/Rev.1" (PDF).

U.S. EIA International Energy Statistics. (2016, Januaray 13). Retrieved from http://www.eia.gov/

Van, Decker, G.W.E., Hollands, K.G.T., & Brunger, A.P. (2001). Heatexchange relations for unglazed transpired solar collectors with circular holes on a square or triangular pitch. *Solar Energy*. 71, 33–45.

Varshney, L., & Saini, J. S. (1998). Heat transfer and friction factor correlations for rectangular solar air heater duct packed with wire mesh screen matrices. *Solar Energy*. 62, 255-262.

Wang, C., Guan, Z., Zhao, X., & Wang, D. (2006). Numerical Simulation Study on Transpired Solar Air Collector. Shenzhen, China: Proceedings of the Sixth International Conference for Enhanced Building Operations (ICEBO).

What Are Greenhouse Gases? . US Department of Energy. (2015, September 11). Retrieved from http://www.eia.gov/oiaf/1605/ggccebro/chapter1.html

Yang, M., Wan,g P., Yang, X., & Shan, M. (2012). Experimental analysis on thermal performance of a solar air collector with a single pass. *Building and Environment*. 56, 361-369.

Yeh, H.M., Ho, C.D., & Hou, J.Z. (2002). Collector efficiency of double-flow solar air heaters with fins attached. *Energy*. 27, 715–727.

Yeh, H., & Ho, C. (2009). Effect of external recycle on the performances of flat-plate solar air heater with internal fins attached. *Renewable Energy*. 34, 1340–1347.

Zenghui, Zhao, Yoav, Peles , & Michae,l K. J. (2013). Properties of plain weave metallic wire mesh screens. *International Journal of Heat and Mass Transfer*. 57, 690-697.